

1. MODIFICATIONS TO THE
FIELD WIND WEIGHTING AND IMPACT PREDICTION
PROCEDURE FOR UNGUIDED ROCKETS

Greenbelt, Md. NASA,
KEITH HENNIGH (N-Mex. State U.)

1711712
PHYSICAL SCIENCE LABORATORY
NEW MEXICO STATE UNIVERSITY
University Blvd.

3 DECEMBER 1963

51p rfs

PREPARED FOR THE
NASA GODDARD SPACE FLIGHT CENTER
NASA CONTRACT NO. NAS 5-3318

~~18500~~

ABSTRACT

A

A study of impact results of Aerobee 150A launchings at Wallops Island, Virginia has resulted in a significant improvement to impact prediction techniques.

NOT FOR

INTRODUCTION

The discussion to be presented is an extension and modification of the impact prediction procedure as reported in "Field Wind Weighting & Impact Prediction Procedure for Unguided Rockets", Ref. (1).

Data collected from Wallops Island, Virginia in support of forty three Aerobee launchings have been used most effectively in detecting biases in impact results and in confirming this new system.

The significant changes to the technique described in Ref. (1) are:

- (a) An additional vector quantity required to transform the wind displacement effect from an inertial reference frame to one relative to a moving launch site on the earth.
- (b) The addition of one term to the wind velocity measurements which transforms the wind velocities from a moving reference frame to an inertial frame.
- (c) A redefinition of the unit wind effect (δ' -matrix) which makes a distinction between a "head" wind and "tail" wind relative to the tower azimuth direction.
- (d) Replacement of the constant coriolis vector by one which is dependent on azimuth and range.
- (e) The combining of all theodolite measurements in evaluating the ballistic wind.

Section I of this report describes the procedure, developing in detail only those terms and definitions which are different than that of Ref. (1). Section II presents evidence of the impact results which validates the proposed changes.

SECTION I

MODIFICATIONS TO WIND VELOCITY PROFILES

Wind Velocity Calculations

The methods of deriving wind velocity component profiles from observations made on theodolite tracking of a piball balloon are identical to that of Ref. (1).

The current practice in computing wind velocity components of a balloon tracked by radar is to use first differences of observed positions. In vector notation the equation

$$\vec{w}_i = \frac{\vec{r}_{i+1} - \vec{r}_i}{t_{i+1} - t_i} \quad (1)$$

represents the average velocity of the balloon in an altitude stratum bounded by the altitudes Z_{i+1} and Z_i .

This definition of a wind velocity is in conflict with its application to the aerodynamic response of the rocket. The conventional wind weighting function, $f(z)$, and unit wind effect, $\delta(\theta)$, are computed relative to an inertial reference frame. Winds computed by equation (1) are referenced to an earth moving frame with origin at the radar. The instantaneous velocity is given by

$$\vec{w}_I = \vec{w}_E + \vec{\omega} \times \vec{r}, \quad (2)$$

where \vec{w}_I is the wind velocity relative to an inertial frame,

\vec{w}_E is the wind velocity relative to an earth fixed frame,

$\vec{\omega}$ is the angular velocity of the earth and

\vec{r} is the position vector of the balloon.

The velocity \vec{w}_I should be used in association with impact prediction work.

In a form suitable for finite differences equation (2) becomes

$$\vec{w}_I = \frac{\vec{r}_{i+1} - \vec{r}_i}{t_{i+1} - t_i} + \vec{\omega} \times \frac{\vec{r}_i + \vec{r}_{i+1}}{2} . \quad (3)$$

The second term uses the average of two consecutive observations of \vec{r} .

It applies equally well to theodolite data; however, the contribution is insignificant. The effect on the wind velocity profile is greatest for large \vec{r} . Table (1) shows the comparison of velocities computed by equations (1) and (3) for Aerobee 4.05, 27 May 1960, radar release No. 1. It is a random choice and in no way represents an extreme.

The application of this term shifts the predicted impact of Aerobee rockets a nominal 1.5 nautical miles in a general westerly direction. The maximum shift observed for 20 rockets is 2.0 nautical miles. This small change may appear insignificant. It has, however, contributed to a much improved impact dispersion and should be considered.

Combining Technique

The current method of combining data from separate balloon tracking missions provides for a permanent change in the profile in terms of successive radar releases. It does not provide a means of retaining winds from previous theodolite releases which may have exceeded, in altitude, the release under current consideration. The effect of discarding the entire previous theodolite with replacement by older radar wind values is detected in a scatter of successive impact calculations. Since it is virtually impossible to expect pi-ball balloons to possess a common rise rate (or to achieve the same vertical displacement in an equal time period) the extent of vertical coverage can not be pre-determined.

TABLE 1

Comparison of velocity components as computed in inertial and earth moving reference frame. Radar Release No. 1, Aerobee 4.05, 27 May 1960.

Z ft.	\dot{X} ft./sec.		\dot{Y} ft./sec.		\dot{Z} ft./sec.	
	Earth	Inertial	Earth	Inertial	Earth	Inertial
640	16.0	15.9	-6.6	-6.6	10.6	10.6
1400	15.6	15.6	-5.5	-5.4	12.6	12.7
2120	11.8	11.7	-1.5	-1.3	12.0	12.1
3630	13.4	13.2	1.5	1.7	12.5	12.7
4390	6.6	6.4	5.6	5.8	12.6	12.9
5105	.6	.3	5.6	5.8	11.9	12.1
5870	-1.5	-1.8	6.3	6.5	12.7	13.0
6600	-.5	-.9	11.1	11.3	12.1	12.4
7400	-8.7	-9.2	13.5	13.6	13.3	13.5
8080	-5.1	-5.7	18.1	18.3	11.3	11.5
8900	-16.3	-16.9	23.3	23.4	13.6	13.8
9660	-19.1	-19.9	18.3	18.4	12.6	12.7
10460	-15.3	-16.1	19.8	19.8	13.3	13.3
11210	-21.6	-22.6	18.8	18.8	12.5	12.5
12000	-17.0	-18.0	22.1	22.1	13.1	13.0
12800	-17.6	-18.8	21.8	21.7	13.3	13.2
14350	-11.9	-13.2	18.0	17.9	12.9	12.7
15050	-18.6	-20.0	14.5	14.2	11.6	11.3
15910	-17.3	-18.8	22.0	21.7	14.3	13.9
16840	-18.1	-19.8	22.0	21.6	15.5	15.1
18420	-14.0	-15.8	10.2	9.8	13.1	12.6
19750	-15.0	-16.9	20.8	20.3	11.0	10.5
20920	-33.3	-35.5	50.0	49.4	9.7	9.0
22520	-46.6	-49.2	49.1	48.3	13.3	12.3
26520	-64.8	-67.9	36.6	35.3	13.3	11.5
30420	-65.8	-69.5	28.6	26.4	13.0	10.1
34420	-67.3	-71.6	28.0	24.8	13.3	9.3
39120	-59.3	-64.3	37.0	33.0	15.6	10.5
43420	-37.3	-43.1	33.3	28.7	14.3	8.3
48320	-84.6	-91.1	33.3	27.8	16.3	9.3
53220	-22.6	-29.7	16.0	9.8	16.3	8.4
58320	-129.3	-136.8	.6	-6.5	17.0	7.7

The new method of combining winds is to extend to theodolite data, the same rules that apply to radar data, hence, retaining any values associated with an earlier theodolite observation not achieved by the current release. By this procedure the quality of wind measurements in the region of 2000 to 4000 feet is improved.

IMPACT CALCULATIONS

Figure 1 depicts the impact geometry.

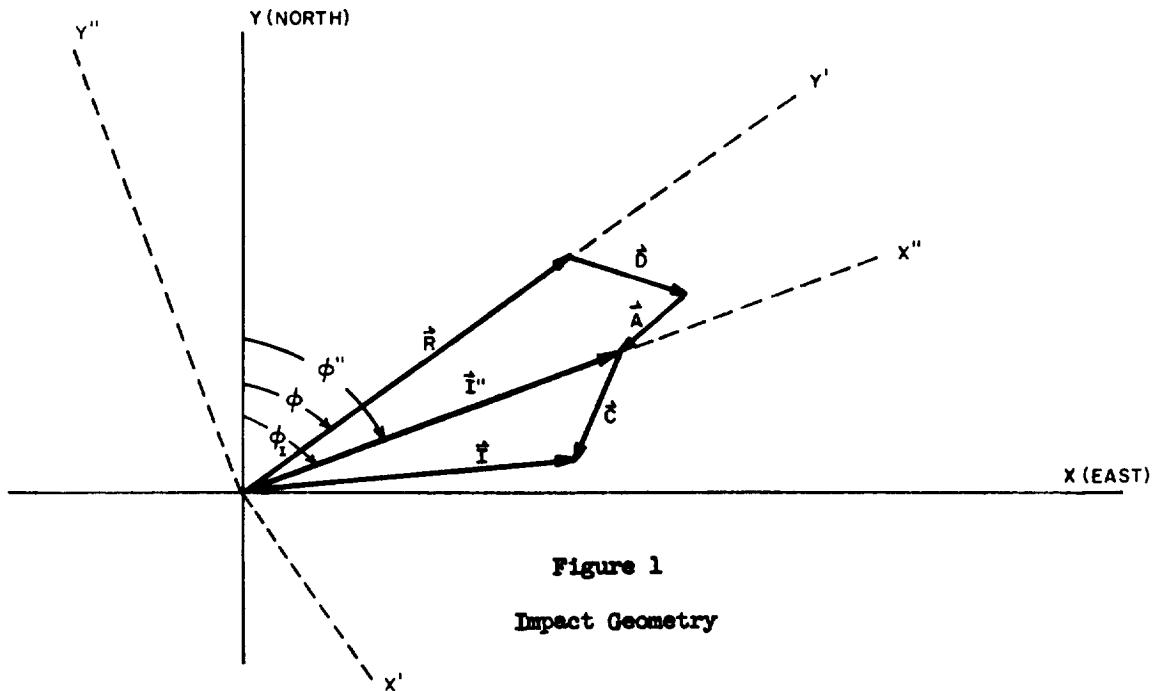


Figure 1
Impact Geometry

The vectors shown are:

- \vec{R} no wind inertial impact point,
- \vec{D} inertial wind displacement vector,
- \vec{A} wind transformation vector,
- \vec{I}'' intermediate impact vector,
- \vec{C} "coriolis vector" and
- \vec{I} final impact vector.

The angles ϕ and ϕ'' are the tower and intermediate azimuth values measured clockwise from north.

The problem to be solved in the impact calculation is expressed by the two vector equations

$$\vec{I}'' = \vec{R} + \vec{D} + \vec{A} \quad (4)$$

and

$$\vec{I} = \vec{I}'' + \vec{C}. \quad (5)$$

The two step solution is used since the value of \vec{I}'' provides necessary arguments for evaluating vector \vec{C} . Justification for this approach will be given in detail at the appropriate time in the following discussion.

Derivations of the terms of equation (4) will now be presented.

The rotation matrix, which translates vector quantities from the unprimed to the primed (tower oriented) coordinate system of Figure (1) is

$$M = \begin{pmatrix} \cos \phi & -\sin \phi \\ \sin \phi & \cos \phi \end{pmatrix} \quad (6)$$

M will be used several times in the following discussion.

Evaluation of \vec{R}

The magnitude of \vec{R} is a function of the tower tilt angle, θ . It is an empirical function best presented as a table of values for $R(\theta)$. Graph 1 represents a typical Aerobee $R(\theta)$ function. The tower azimuth angle, ϕ , is required to form

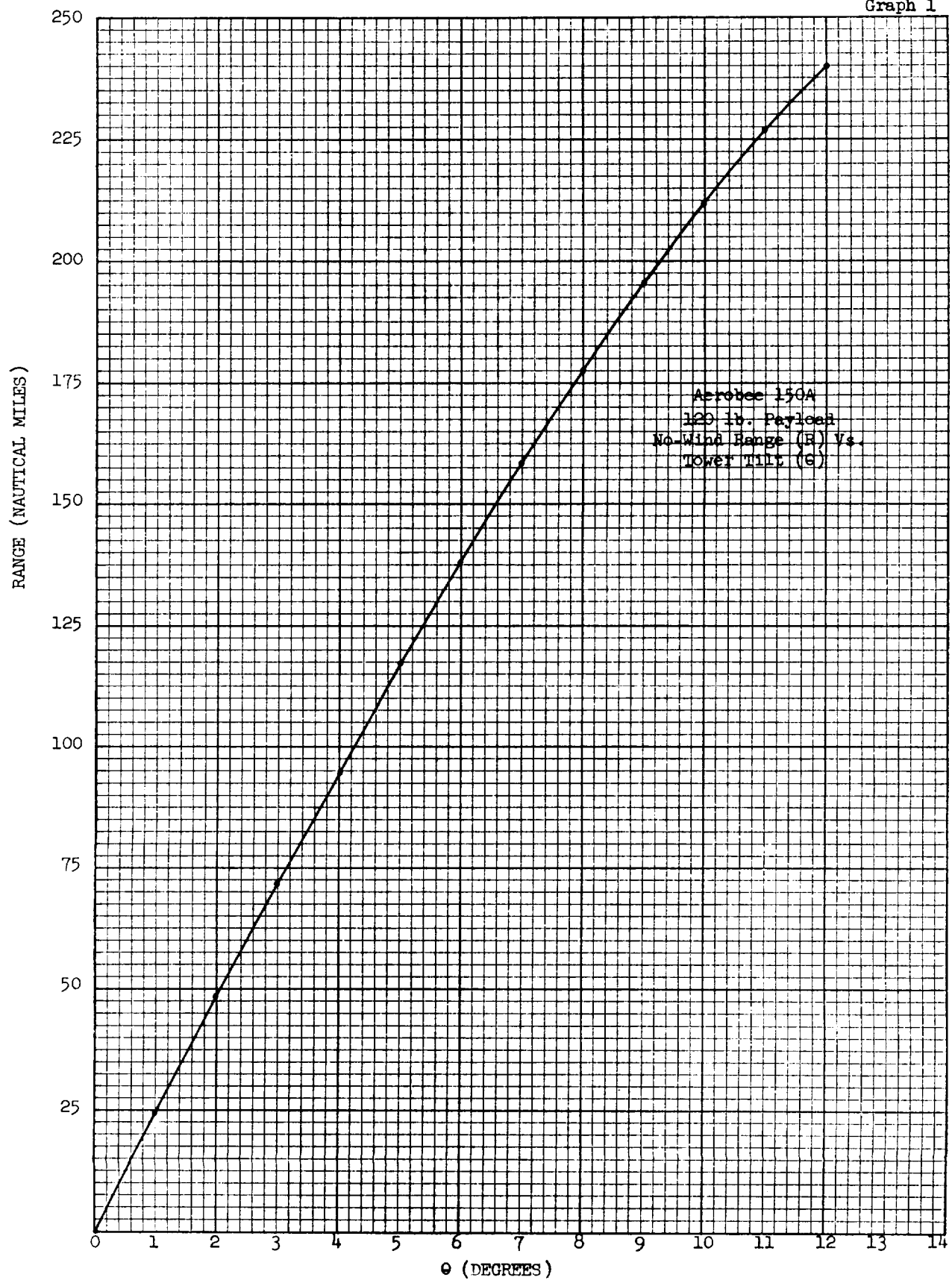
$$\vec{R}(\theta, \phi) = M^{-1} \vec{R}'(\theta) \quad (7)$$

where

$$\vec{R}'(\theta) = \begin{pmatrix} 0 \\ R(\theta) \end{pmatrix}.$$

Equation (7) expresses the no-wind, inertial impact point in the unprimed coordinate system. The derivation is consistent with Ref. (1).

Graph 1



Evaluation of \vec{D}

\vec{D} is the displacement vector of the rocket resulting from the wind. It is expressed by

$$\vec{D} = M \delta' M^{-1} \vec{W} \quad (8)$$

where

$$\delta' = \begin{pmatrix} \delta_c(\theta) & 0 \\ 0 & \delta_R(\theta) \end{pmatrix}. \quad (9)$$

The familiar ballistic wind vector

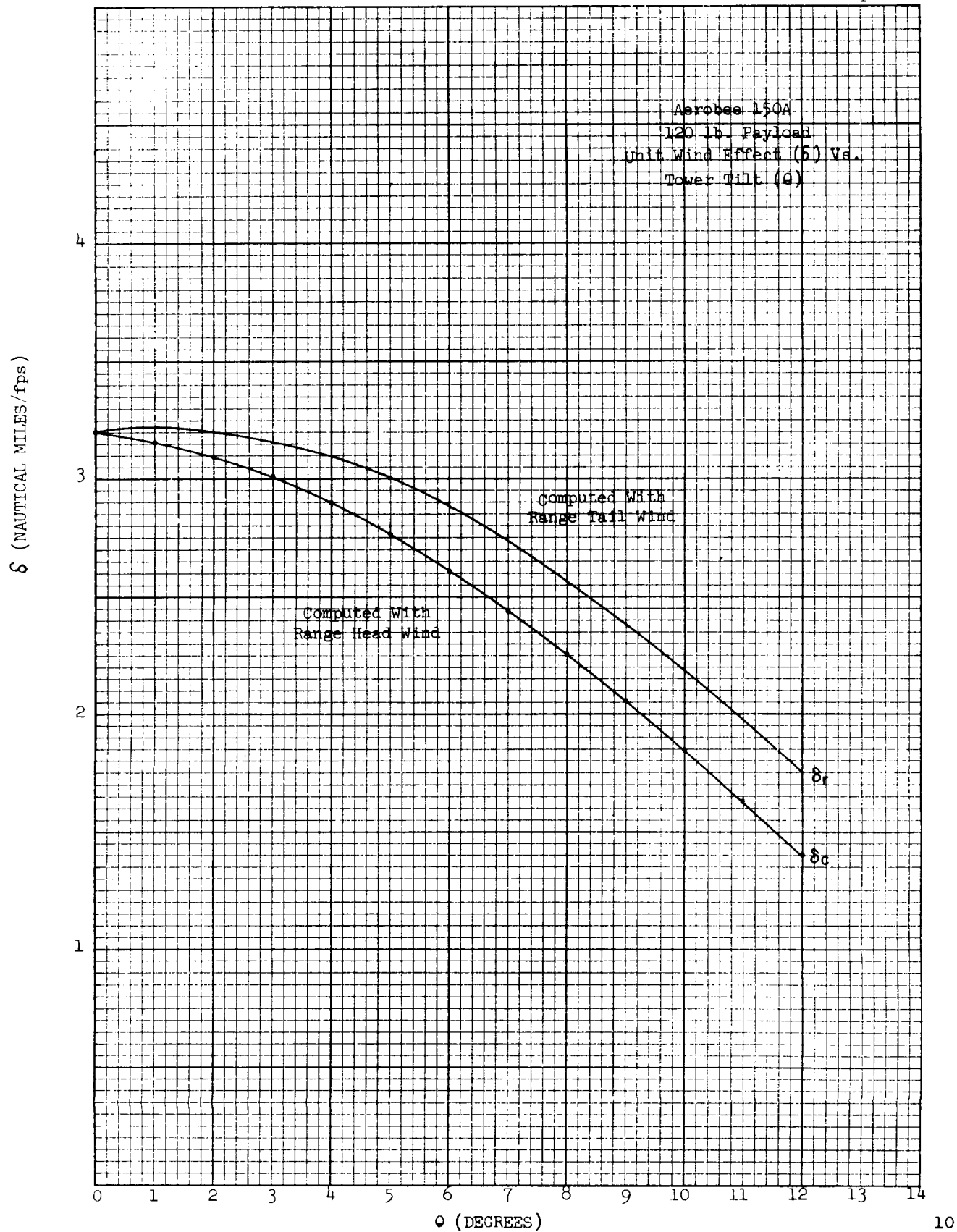
$$\vec{W} = \begin{pmatrix} W_x \\ W_y \end{pmatrix}, \quad (10)$$

is created by summing wind velocity components with a wind weighting function. The algebraic sign of the ballistic wind is reversed to that of the actual wind, Ref. (1). The two values expressed in the δ' -matrix are the unit wind effects relative to the cross and range wind components as seen in the primed (tower) system.

A distinction can be made between the values of δ_c and δ_R . Simulation studies have revealed a functional dependence of δ on tower tilt, θ , and the algebraic sign of the range wind component.* A tail wind, (a wind in the direction of the tower azimuth) creates a "pitch-up" of the rocket; a head wind creates a "pitch-down". Graph (2) demonstrates this characteristic. Notice also that δ_R is a maximum at a value of θ not equal to zero.

*Studies also indicate the dependence of both $\delta(\theta)$ and $f(t)$ on wind magnitude. If this effect were to be introduced in a manner which first appears feasible, impact errors observed in the forty three rocket samples would yield results less favorable than those resulting by ignoring this effect. Until this is better understood the choice has been made to treat these parameters as independent of wind magnitude. The details of this effect is to be omitted from this report.

Graph 2



Values of $\delta_c(\theta)$ and $\delta_R(\theta)$ are selected from appropriate tables in a manner similar to that of $R(\theta)$.

One additional concept is required in the actual selection of the elements to be used in the δ' -matrix. A cross-wind component acting upon a rocket can have but one effect; that of degrading the overall performance. Stated another way, the cross-wind effect can only result in a pitch-down in terms of the trajectory to be flown. The range wind, on the other hand, can cause the rocket to pitch-up or down in terms of the trajectory. The assumption to be used is that a head-wind has the same effect as a cross-wind, in terms of rocket wind displacement. In the case of a head-wind, the value of $\delta_R(\theta)$ is to be replaced by the value of $\delta_c(\theta)$ and the matrix actually becomes a scalar quantity in its application to equation (8). When a tail-wind exists the value of $\delta_R(\theta)$ remains unchanged. This condition may be restated:

$$\text{if } W_y' > 0, \text{ set } \delta_R(\theta) = \delta_c(\theta). \quad (11)$$

The above assumptions have proven to be a satisfactory approximation to the cross-wind effect.

The similarity transformation indicated in equation (8) transforms the δ' -matrix to the unprimed system.

Evaluation of \vec{A}

The vector \vec{A} is a quantity previously ignored in all known wind impact prediction theories. Its development is an outgrowth of attempting to explain an impact bias observed in rocket impacts over an extended period of time.

In order to best understand the concept, consider first, in the simplest possible form, the development of a coriolis displacement vector. In simula-

tion work the impact of a rocket is calculated in an inertial and then in an appropriate earth-moving reference frame.

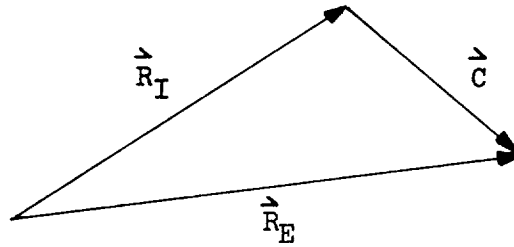


Figure 2

(Coriolis Displacement Vector)

From Figure 2, the equation

$$\vec{R}_E = \vec{R}_I + \vec{C}, \quad (12)$$

is a transformation of the rocket impact from an inertial to an earth moving frame.

The vector \vec{A} is a similar transformation which operates on the wind displacement vector \vec{D} . Consider equation (8),

$$\vec{D} = M \delta' M^{-1} \vec{W},$$

and the definition of the ballistic wind,

$$\vec{W} = \int_0^{Z_{\max}} \frac{d [f(z)]}{dz} \vec{w}(z) dz, \quad (13)$$

where $f(z)$ is a wind weighting function and $\vec{w}(z)$ is the wind profile as computed by equation (3) with the algebraic sign reversed. This reversal of sign is required to properly compute the direction of rocket response.

Inspection reveals that all quantities involved apply to an inertial frame. However, the rocket is to be launched in a reference frame moving with the earth. A similar diagram to that of Figure 2 may be drawn to represent the velocity components of the rocket at a given instant of time (or altitude, Z) for the inertial and the moving frames.

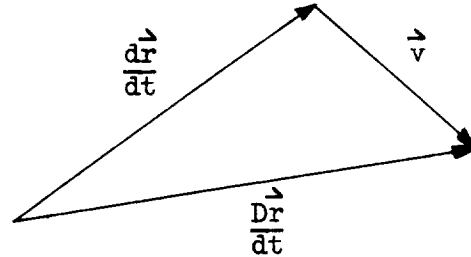


Figure 3

(Velocity Transformation Diagram)

From Figure 3, the equation

$$\vec{v}(z) = \vec{\frac{Dr}{dt}} - \vec{\frac{dr}{dt}} \quad (14)$$

represents the difference between the velocity as seen in the two reference frames. The notation, D, indicates a derivative with respect to the moving frame and, d, a derivative with respect to the inertial frame, Ref. (2), page 208.

The equation

$$\vec{\frac{dr}{dt}} = \vec{\frac{Dr}{dt}} + \vec{\omega} \times \vec{r}. \quad (15)$$

expresses the transformation from the earth reference frame to the inertial frame. Combining yields

$$\vec{v}(z) = -\vec{\omega} \times \vec{r}(z), \quad (16)$$

a quantity which, when added to the inertial winds transforms these winds to an earth moving frame. The algebraic sign in equation (16) is correct for the ballistic wind application, i.e., the rocket will respond in the indicated direction.

This transformation is expressed by the equation

$$\begin{aligned}\vec{w}(z) &= -\vec{w}_I(z) + \vec{v}(z) \\ &= -\vec{w}_I(z) - \vec{\omega} \times \vec{r}(z).\end{aligned}\tag{17}$$

The term $\vec{w}_I(z)$ are those values computed from equation (3) with the algebraic sign reversed.

Substituting equation (17) into equation (13) yields

$$\begin{aligned}\vec{W} &= \int_0^{Z_{\max}} \frac{d[f(z)]}{dz} \vec{w}(z) dz \\ &= - \int_0^{Z_{\max}} \frac{d[f(z)]}{dz} \vec{w}_I(z) dz - \int_0^{Z_{\max}} \frac{d[f(z)]}{dz} \vec{\omega} \times \vec{r}(z) dz \\ &= \vec{W}_I + \vec{W}_R.\end{aligned}\tag{18}$$

The first term, \vec{W}_I , is the regular ballistic wind velocity and the second, \vec{W}_R , is a term which transforms the ballistic wind into a moving frame. By substituting into equation (8), the wind displacement vector decomposes into two vectors, viz.,

$$\vec{D}_T = M \delta' M^{-1} (\vec{W}_I + \vec{W}_R)$$

or

$$\vec{D}_T = \vec{D} + \vec{A}\tag{19}$$

where

\vec{D}_T represents the total wind displacement.

\vec{D} represents the measured wind effect in the inertial frame.

\vec{A} represents the transformation of \vec{D} to a moving reference frame.

The similarity to the coriolis transformation, equation (12), is apparent.

Although \vec{v} has a vertical component of velocity, the definition of δ' provides only for establishing wind effects of the horizontal components and no use has been made of the vertical component. The values of \vec{W}_R are functions of θ and ϕ . Graphs 3 and 4 are typical component curves for an Aerobee 150A.

The vector \vec{A} is the most significant contribution to be presented in this report. In Section II it will be demonstrated that this quantity does remove the impact bias.

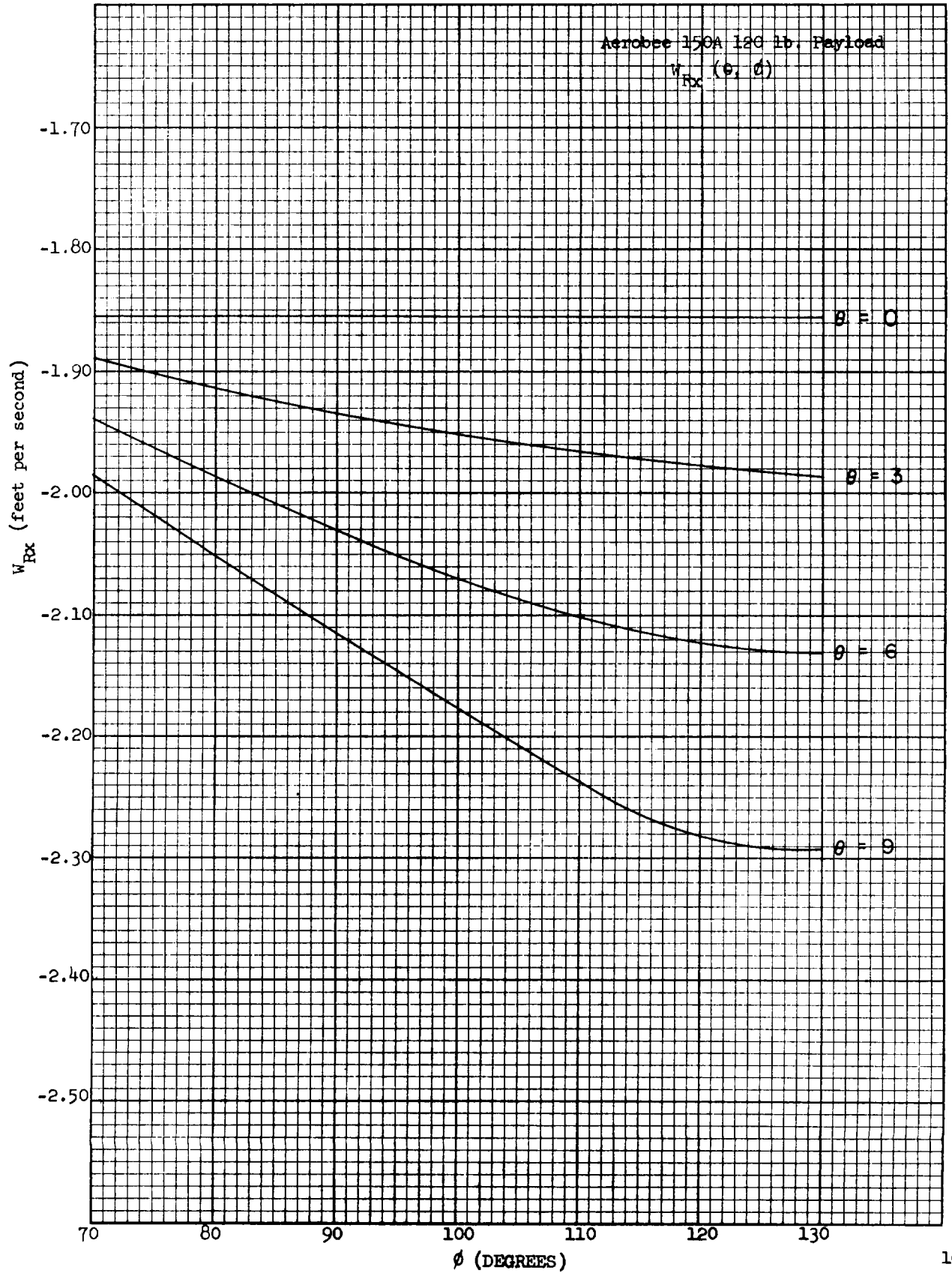
Evaluation of \vec{C}

The so-called "coriolis vector", \vec{C} , represents not only the coriolis displacement, but the displacement due to the centrifugal term and a correction to adjust for the use of a flat earth with inverse square gravity directed along the Z-axis, in the evaluation of equation (4).

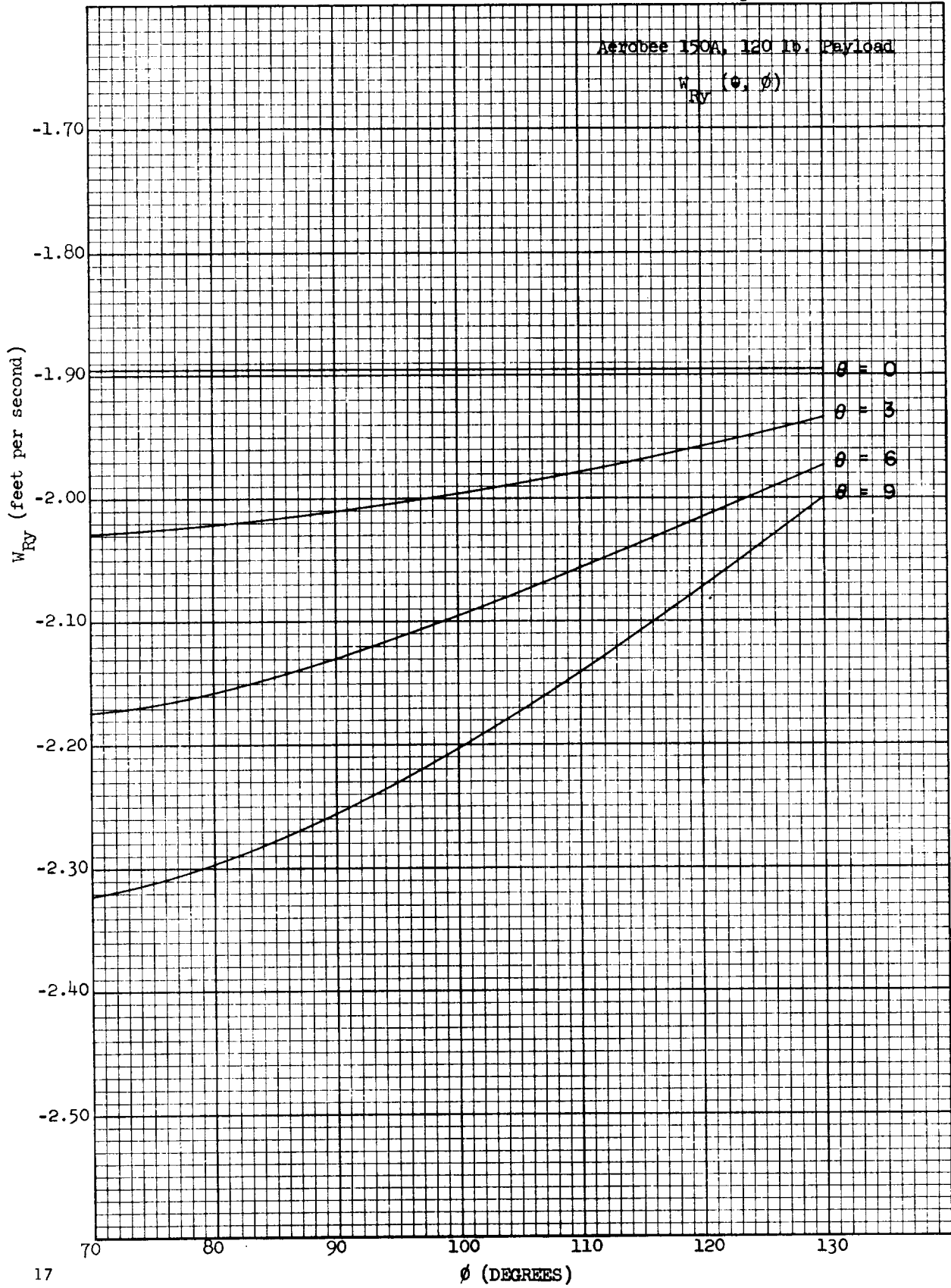
Refer to Figure 4. The unprimed coordinate system with origin at launcher, has the directions east, north, and vertical relative to the plumb line. The double primed system has its X'' -axis directed along the \vec{I} vector of equation (1).*

*The convention of a double primed system is the result of remaining consistent with the simulation programs.

Graph 3



Graph 4



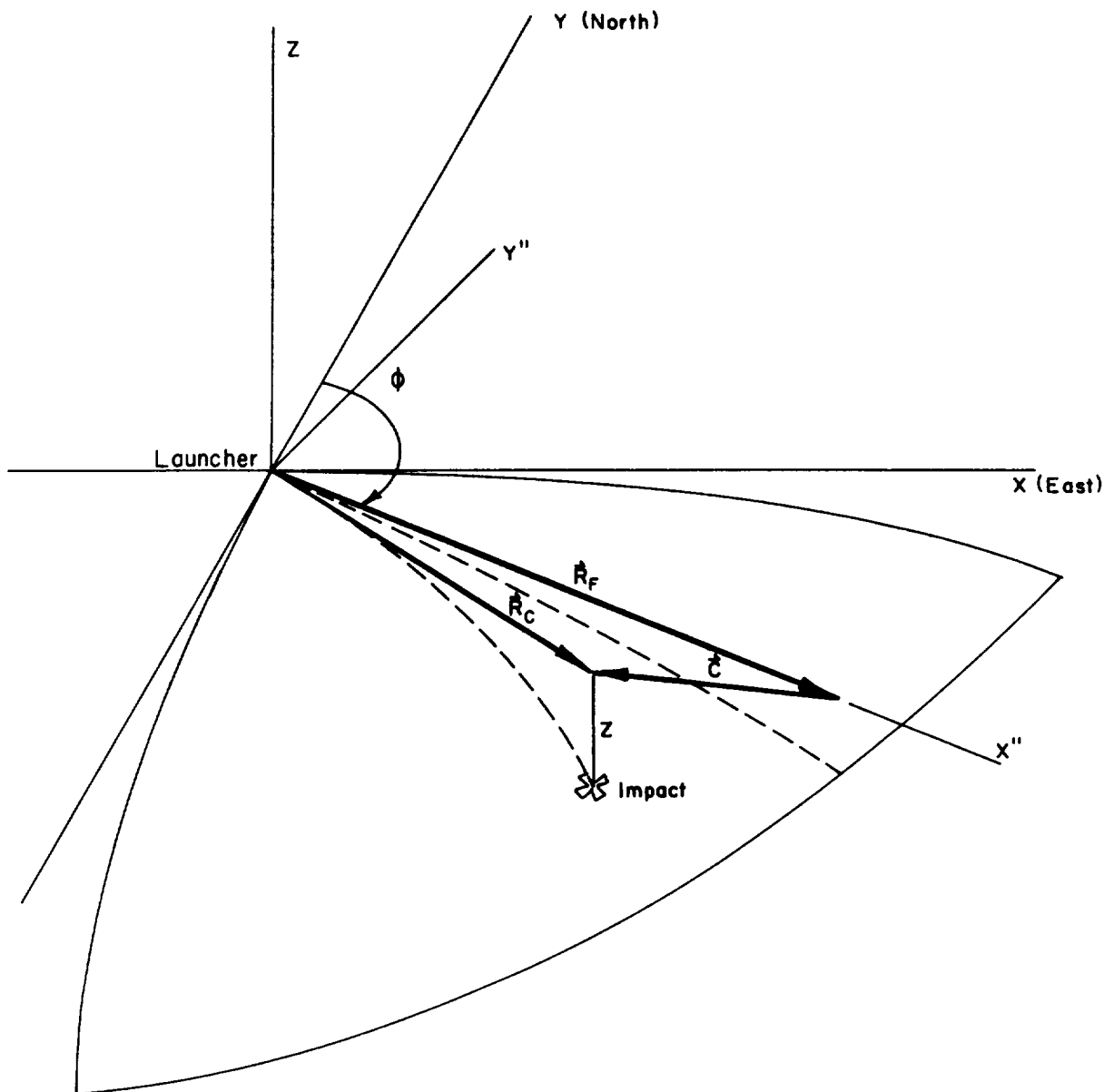


Figure 4
Coriolis Geometry

\vec{R}_F represents the impact vector along X'' axis whose magnitude is equal to the impact displacement computed with a particle trajectory in a flat earth model. \vec{R}_C represents the point where a curved earth particle impact projects onto the horizontal plane; the original launch azimuth in this simulation being defined by ϕ . The "coriolis vector" is defined to be

$$\vec{C} = \vec{R}_C - \vec{R}_F . \quad (20)$$

The application of \vec{C} is by an indirect method which will now be explained.

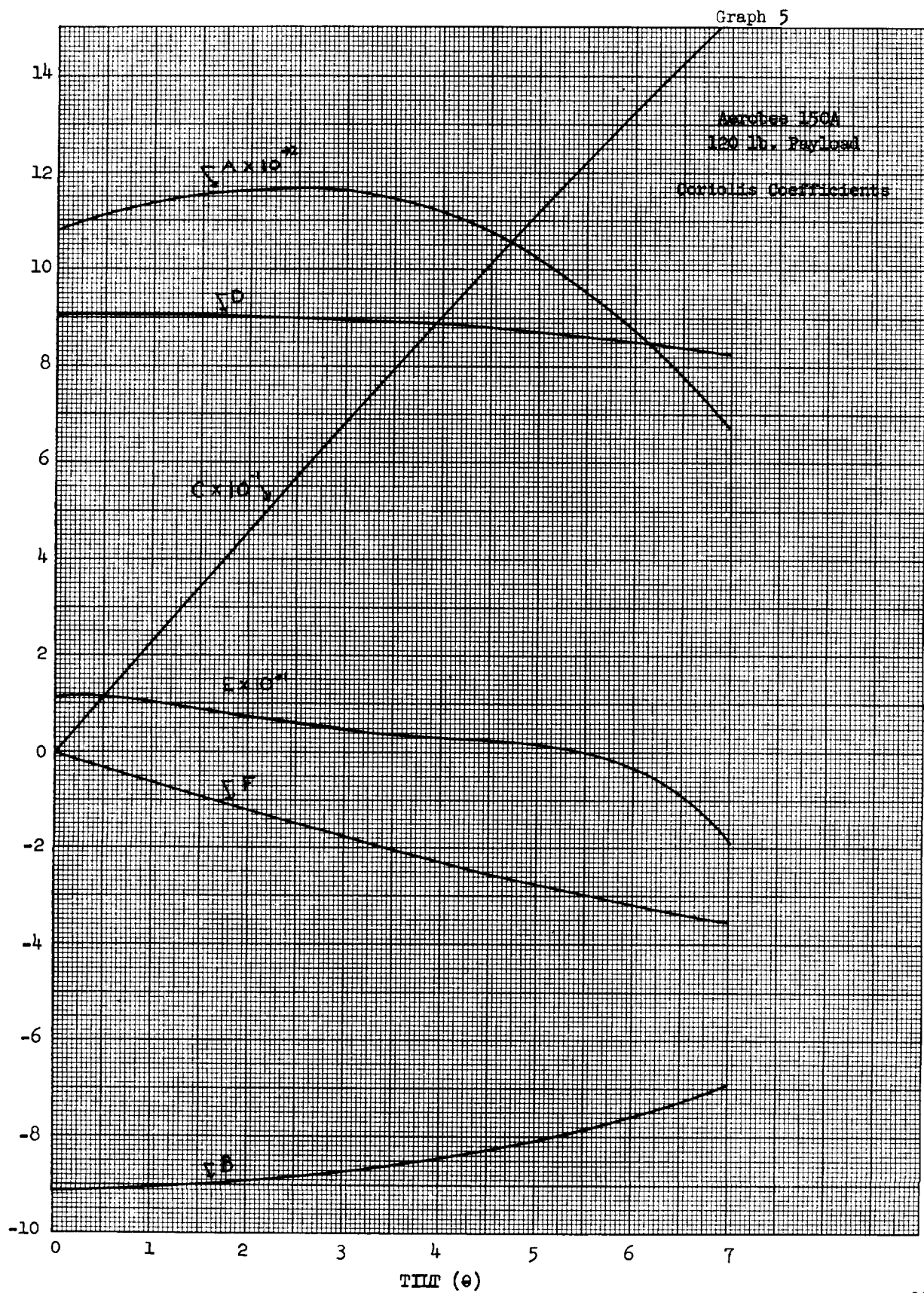
Inspection of the components of \vec{R}_C , as computed in the double primed coordinate system, holding θ constant with variation on ϕ reveal that the values may be mapped through the full range $0 \leq \phi < 360$. By computing for three firing azimuths which envelope the planned or nominal trajectory, sufficient data are available to evaluate coefficients of the equations:

$$\begin{aligned} I_{x''} &= A(\theta) \cos \phi + B(\theta) \sin \phi + C(\theta) \\ I_{y''} &= D(\theta) \cos \phi + E(\theta) \sin \phi + F(\theta). \end{aligned} \quad (21)$$

With variation in θ , a series of coefficients are computed and these coefficients $A(\theta)$, $B(\theta)$, etc., are functions of θ . Graph 5, demonstrates a typical set of coefficients.

It is to be noted that neither the components of \vec{C} nor \vec{R}_C expressed in the unprimed coordinate system possess such convenient forms for an empirical fit.

Test cases have been produced in which three nominal values of ϕ were used to construct the required coefficients of equation (21). Additional values of ϕ were calculated through the zero to 360 degree range. Excellent



agreement was found with the maximum deviation occurring in the vicinity of 180° removed from nominal azimuth. The following table shows the maximum deviation in $I_{x''}$ and $I_{y''}$ for various payloads.

Table of Comparisons of
Values Obtained by Equations (21) and Simulated Values

Payload (pounds)	θ (degrees)	ϕ (degrees)	X'' Deviation (nautical miles)	Y'' Deviation (nautical miles)
120	12	270	0.202	0.043
200	12	270	0.135	0.030
320	12	270	0.075	0.017

Since θ may be expressed as a function of R_F , the coefficients in equations (21) may also be expressed as functions of R_F . To select the proper coefficients, equation (4) is solved; the magnitude of \vec{I}'' is the equivalent of R_F and ϕ'' is the defined firing azimuth. The decision to use \vec{I}'' for arguments in this derivation is due to the fact that the wind displacement vectors are established early in the flight and the greatest contribution to \vec{C} results from the trajectory which is established from the earlier flight history.

The impact point calculated by equation (21) is expressed in the double primed reference frame. It is necessary to transform these components to the unprimed coordinate system by the equation

$$\vec{I} = \begin{pmatrix} \sin \phi'' & -\cos \phi'' \\ \cos \phi'' & \sin \phi'' \end{pmatrix} \begin{pmatrix} I_{x''} \\ I_{y''} \end{pmatrix} . \quad (22)$$

The above result is the equivalent of solving equation (5).

SUMMARY OF IMPACT CALCULATIONS

Given: (the tower setting (θ, ϕ) and the ballistic wind, \vec{W} . Sequence of operations:

1. Evaluate: $R(\theta)$ from table represented by Graph 1.

$\delta_c(\theta)$ and $\delta_R(\theta)$ from table represented by Graph 2.

W_{Rx} and W_{Ry} from double argument tables represented by Graphs 3, 4, 5, and 6.

2. Compute components of \vec{R} :

$$R_x = R \sin \phi$$

$$R_y = R \cos \phi \quad \text{Eq. (7)}$$

3. Compute components of \vec{W} :

$$W_x = W_{Ix} + W_{Rx}$$

$$W_y = W_{Iy} + W_{Ry} \quad \text{Eq. (19)}$$

4. Compute W'_y :

$$W'_y = -W_x \sin \phi + W_y \cos \phi$$

5. If: $W'_y > 0$ $\delta_c(\theta) \rightarrow \delta_R(\theta)$ ($\delta_R(\theta)$ is set equal to $\delta_c(\theta)$).

6. Compute in components $(\vec{D} + \vec{A})$:

$$(D_x + A_x) = W_x (\delta_c \cos^2 \phi + \delta_R \sin^2 \phi) + W_y (\delta_c - \delta_R) \sin \phi \cos \phi$$

$$(D_y + A_y) = W_x (\delta_c - \delta_R) \sin \phi \cos \phi + W_y (\delta_c \sin^2 \phi + \delta_R \cos^2 \phi). \quad \text{Eq. (8)}$$

7. Sum Components:

$$\begin{aligned}
 I''_x &= R_x + (D_x + A_x) \\
 I''_y &= R_y + (D_y + A_y) \\
 I'' &= \sqrt{I''_x^2 + I''_y^2} \\
 \phi'' &= \tan^{-1} \left(\frac{I''_x}{I''_y} \right)
 \end{aligned}
 \tag{Eq. (1)}$$

8. Using I'' as argument evaluate coefficients (Graph 7) of equation (21) and compute:

$$\begin{aligned}
 I_{x''} &= A \cos \phi'' + B \sin \phi'' + C \\
 I_{y''} &= D \cos \phi'' + E \sin \phi'' + F
 \end{aligned}
 \tag{Eq. (21)}$$

9. Rotate to unprimed system

$$\begin{pmatrix} I_x \\ I_y \end{pmatrix} = \begin{pmatrix} \sin \phi'' & -\cos \phi'' \\ \cos \phi'' & \sin \phi'' \end{pmatrix} \begin{pmatrix} I_{x''} \\ I_{y''} \end{pmatrix}
 \tag{Eq. (23)}$$

10. Transform the impact vector, \vec{I} , to polar form:

$$\begin{aligned}
 I &= \sqrt{I_{x''}^2 + I_{y''}^2} \\
 \phi_I &= \tan^{-1} \left(\frac{I_x}{I_y} \right)
 \end{aligned}$$

The double entry tables present some complexity in the reverse solution. The proposed approach is to choose an arbitrary tower setting, compute an impact point using the 10 steps. The difference between the desired impact

and the calculated impact is averaged and the tower setting corrected in tilt and azimuth. The process is repeated until agreement is achieved to some tolerance, ϵ .

SECTION II

DATA CORRELATION

The graphs associated with this section present the results of applying the modified impact theory. A total of forty three Aerobee rockets have been used in this treatment. Nineteen of these rockets were examined in the preliminary study which led to the modifications. The remaining twenty four were then subjected to the developed theory.

The first four polar plots represent the error vectors from the predicted impact point to the impact reported by radar.

Graph 6 represents some results reported from the field operation using the original computational procedure. The data does show a southwest bias in the distribution.

Simulation studies indicated a difference between "head" and "tail" wind effects. It was believed that the cross and range wind effect could contribute to the observed bias. Also there was reason to believe that the "coriolis vector", being treated as constant, could contribute a bias. The new plan to combine theodolite data into the wind profile was introduced.

Graph 7 demonstrates the results of modifying for these conditions. The net result is a closer grouping of the impacts, and with forty three rockets the bias becomes more apparent.

Further considerations suggested the bias was explainable by the earth's rotation rather than wind effect or rocket performance. It had previously been recognized that the radar wind computations were for an earth moving reference frame; however, the effect was believed to be negligible.

Graph 8 is the results of including the inertial transformation term on the winds. A slight improvement is observed.

Subsequent consideration led to the conclusion that the impact prediction was biased because the wind displacement was computed in an inertial reference frame. The vector \vec{A} was introduced to transform the inertial wind displacement vector to a moving frame.

Graph 9 is the final result with all five modifications imposed. In this graph the bias appears to be eliminated.

In order to further examine the bias, averages of these errors were formed in a Cartesian coordinate system. The averages are:

$$\bar{E}_x = 0.68 \text{ nautical miles west}$$

$$\bar{E}_y = 0.59 \text{ nautical miles north}$$

$$|\bar{E}| = 8.48 \text{ nautical miles.}$$

Cumulative distribution plots were formed of these components in order to examine the type of distribution. Graphs 10 and 11 demonstrate a strong tendency toward normal (Gaussian) distribution of the components.

Examination of the distributions in polar form are represented in Graphs 12 and 13. The first is a cumulative plot of the angular values. If these data possess no bias, then the angular values would be expected to be uniformly distributed. The general slope of the cumulative data of Graph 12 demonstrates this uniform distribution. The magnitude of the error vector would be expected to be Rayleigh distributed. The grid of Graph 13 is such that data conforming to a Rayleigh distribution will plot linearly. The expected distribution is well demonstrated in Graph 13.

These averages and distributions demonstrate strong supporting evidence that the theory as developed does provide a suitable method of impact prediction.

Graph 13 is also useful as an empirical dispersion study for the Aerobee 150A rocket. For example: 50% of all rockets fired will be expected to fall within 7.8 nautical miles of the predicted impact. It is interesting to note that previous dispersion studies for the Aerobee 150A show consistent results.

Graph 14 is a bar chart showing the error magnitude in order of firing sequence. It is a first attempt to develop a quality control.

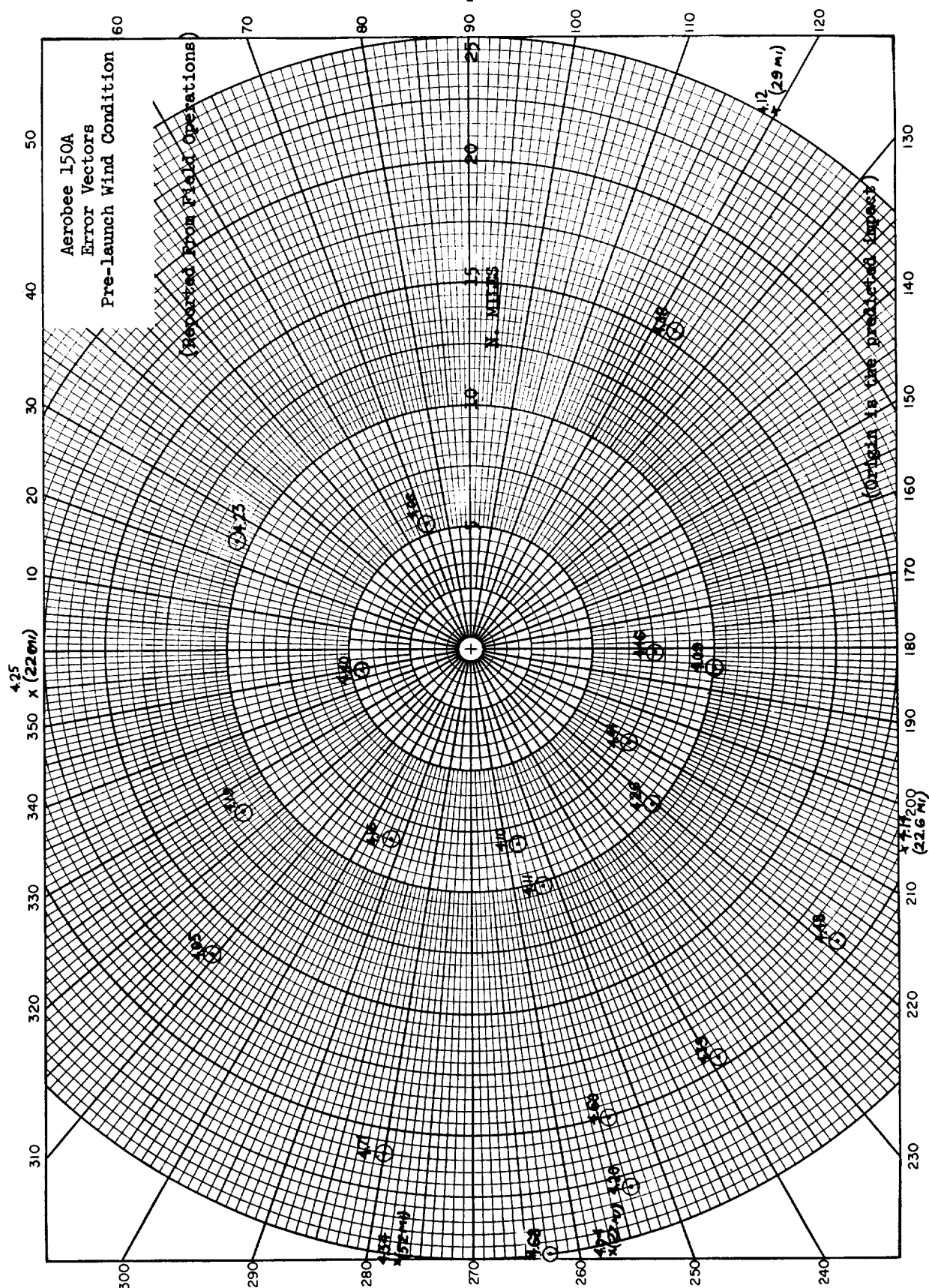
Graph 15 is a bar chart showing the magnitude of the wind displacement vector, $|\vec{D}|$. Its presentation is primarily to demonstrate the types of winds which have been encountered in the firing of these rockets.

Graph 16 plots error magnitude versus ballistic wind magnitude. It is a primitive attempt to correlate wind velocities with miss distance. This graph shows that the error magnitude seems to be independent of ballistic wind magnitude. The results support an argument to gradually increase the upper limit of the ballistic wind magnitude which is permissible for Aerobee launch operations.

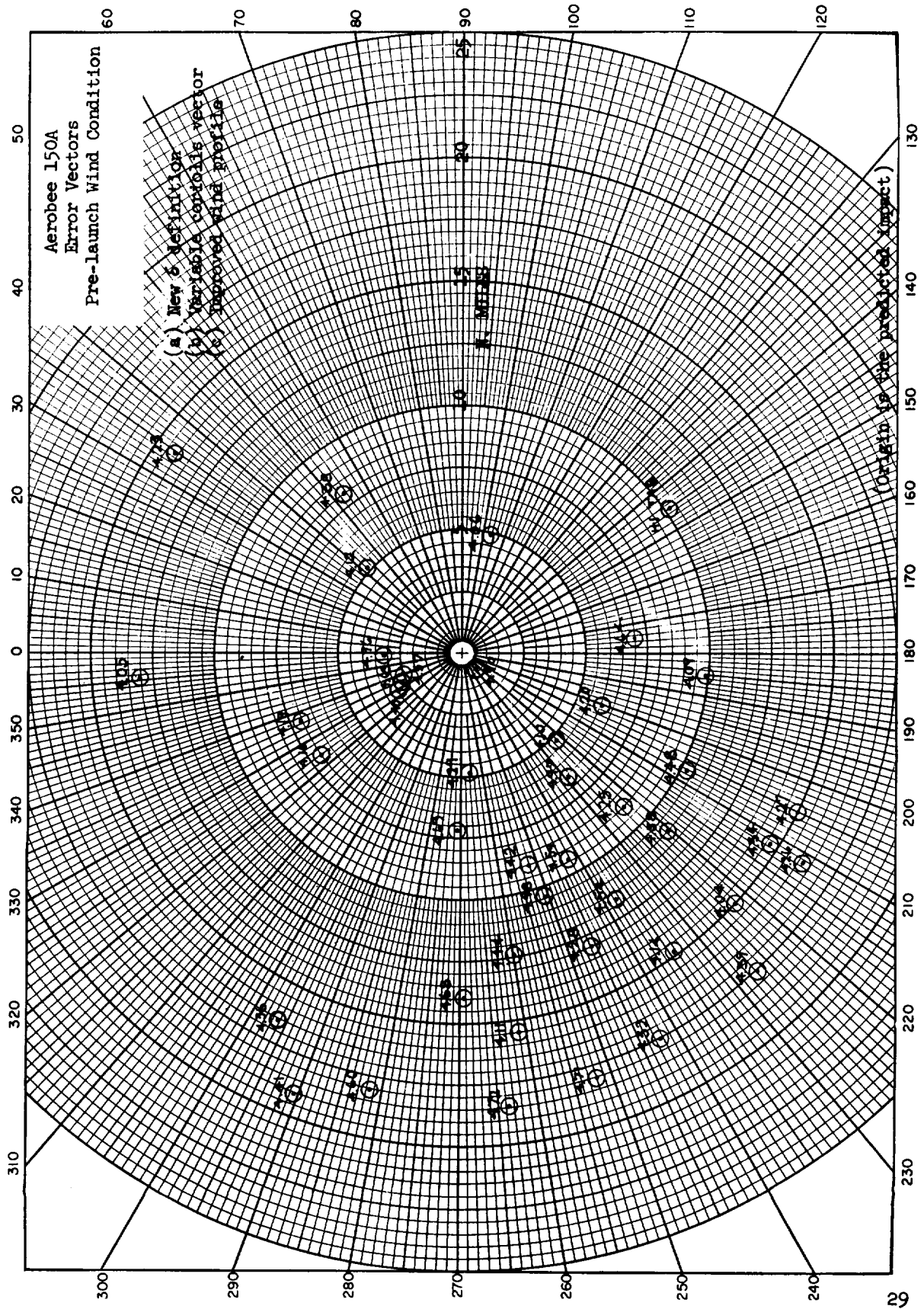
Graphs 17 and 18 are similar plots of error magnitude versus payload weight and tower tilt. They also show little correlation with miss distance.

Additional unnumbered graphs represent similar studies performed with post-flight wind conditions. The results, in general, duplicate those of the pre-flight study.

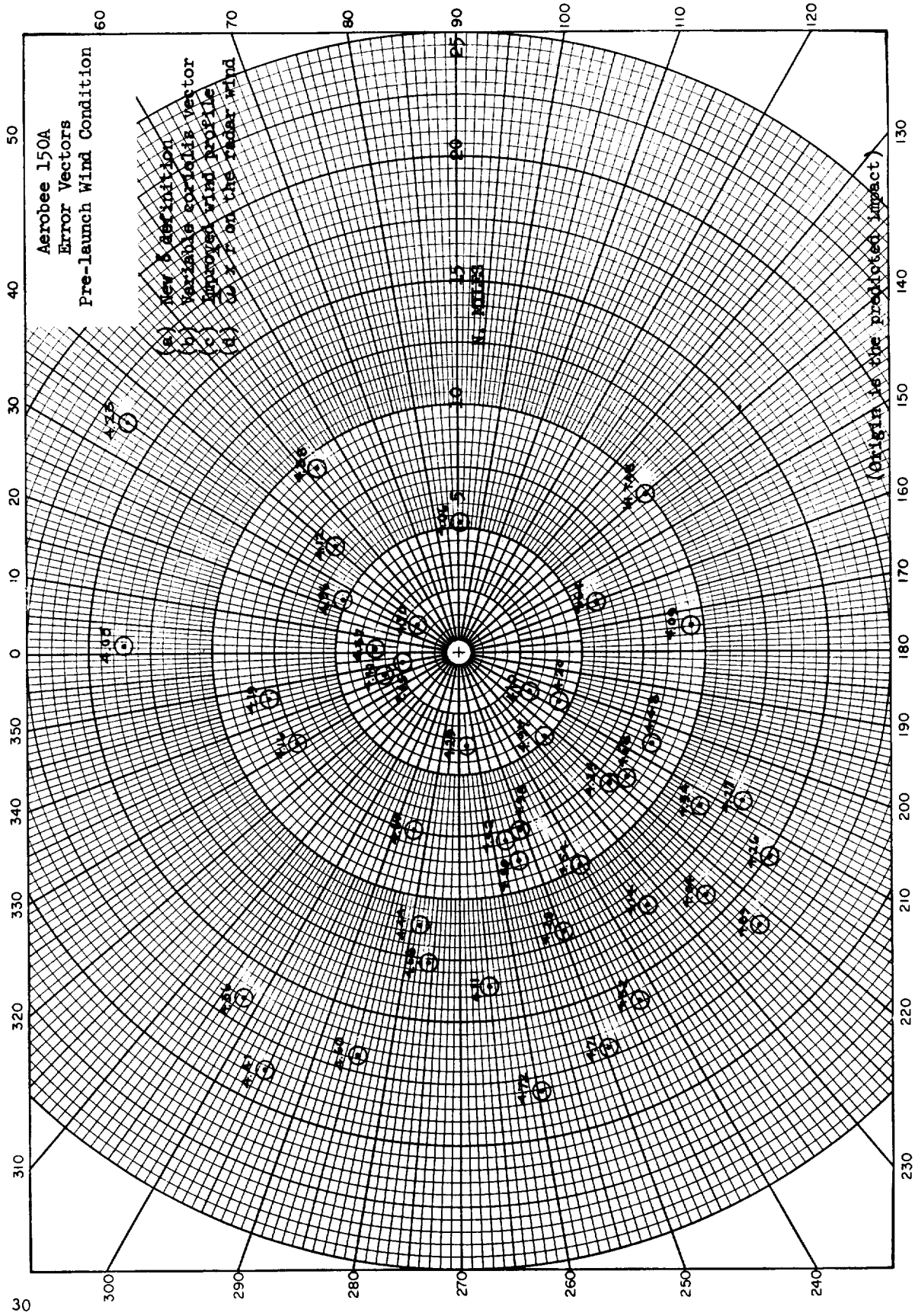
Graph 6



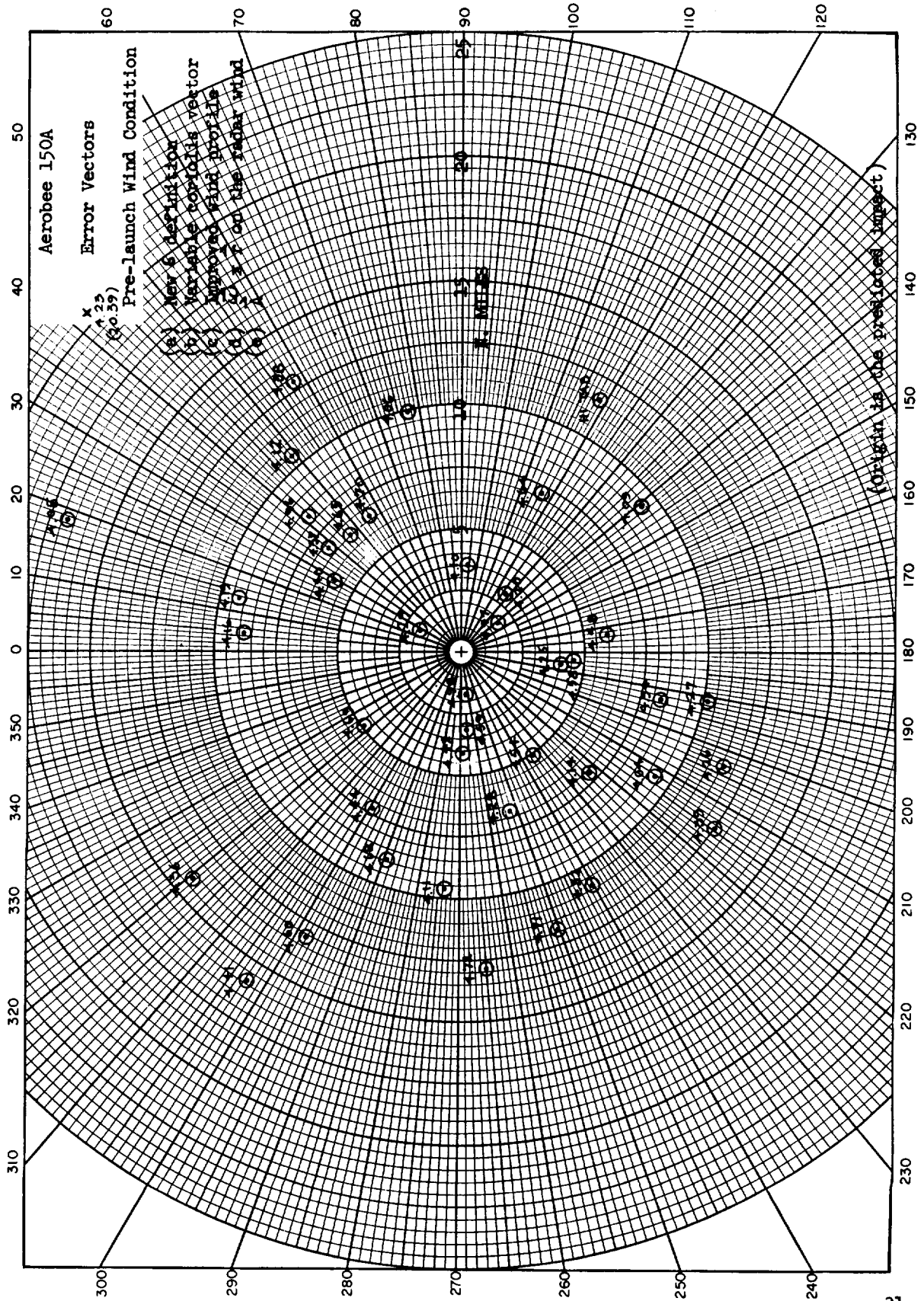
Graph 7



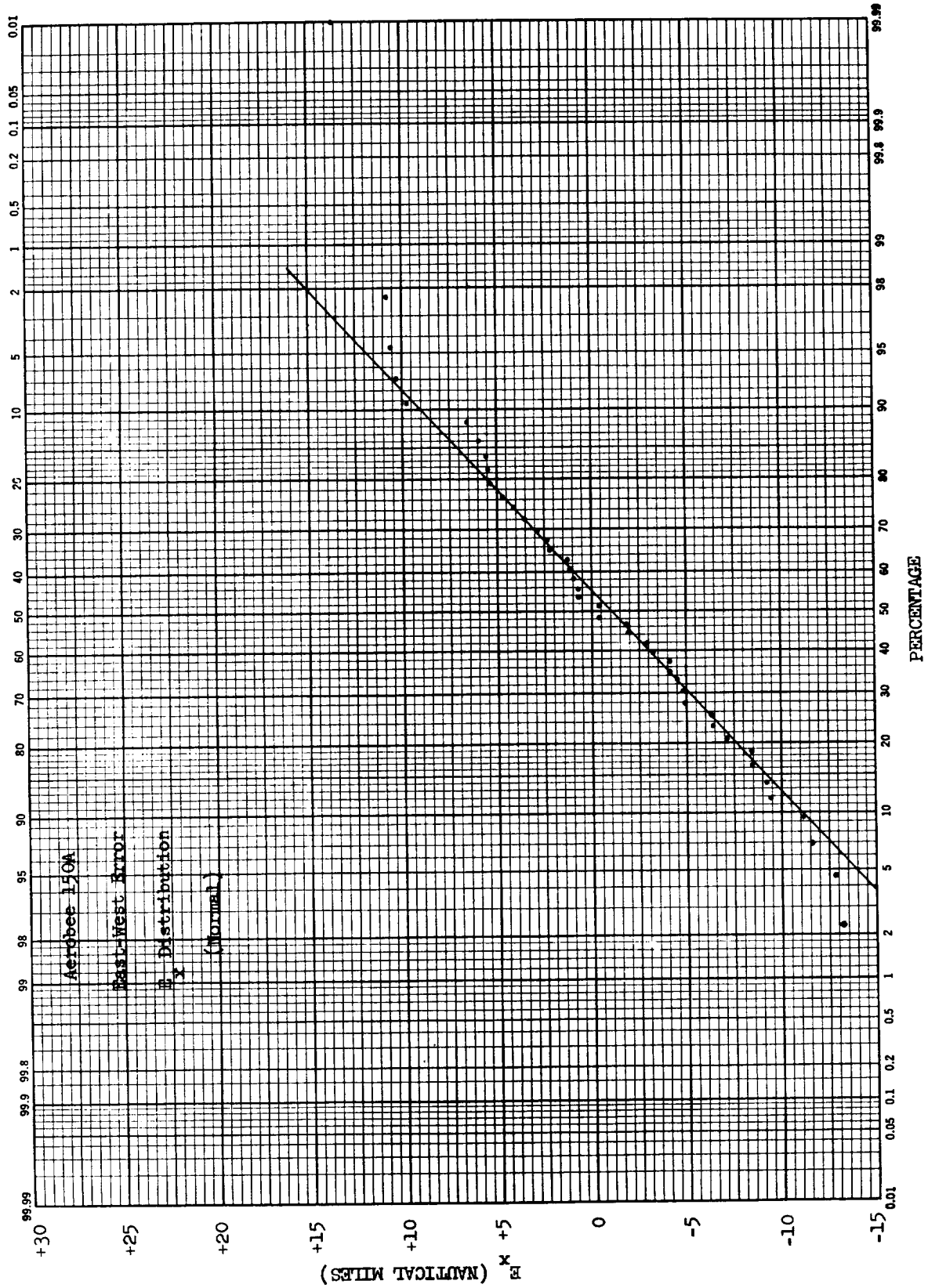
Graph 8



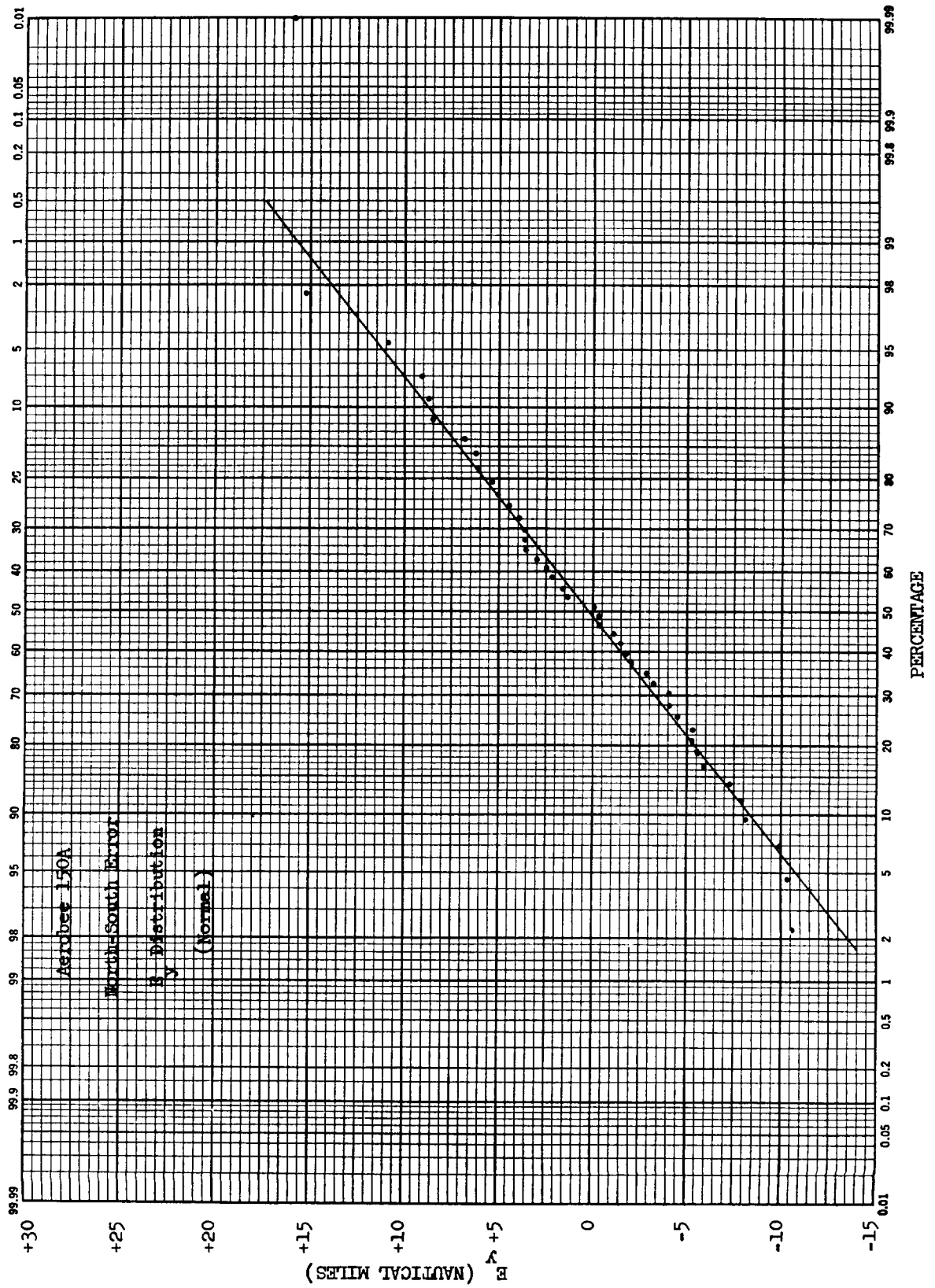
Graph 9



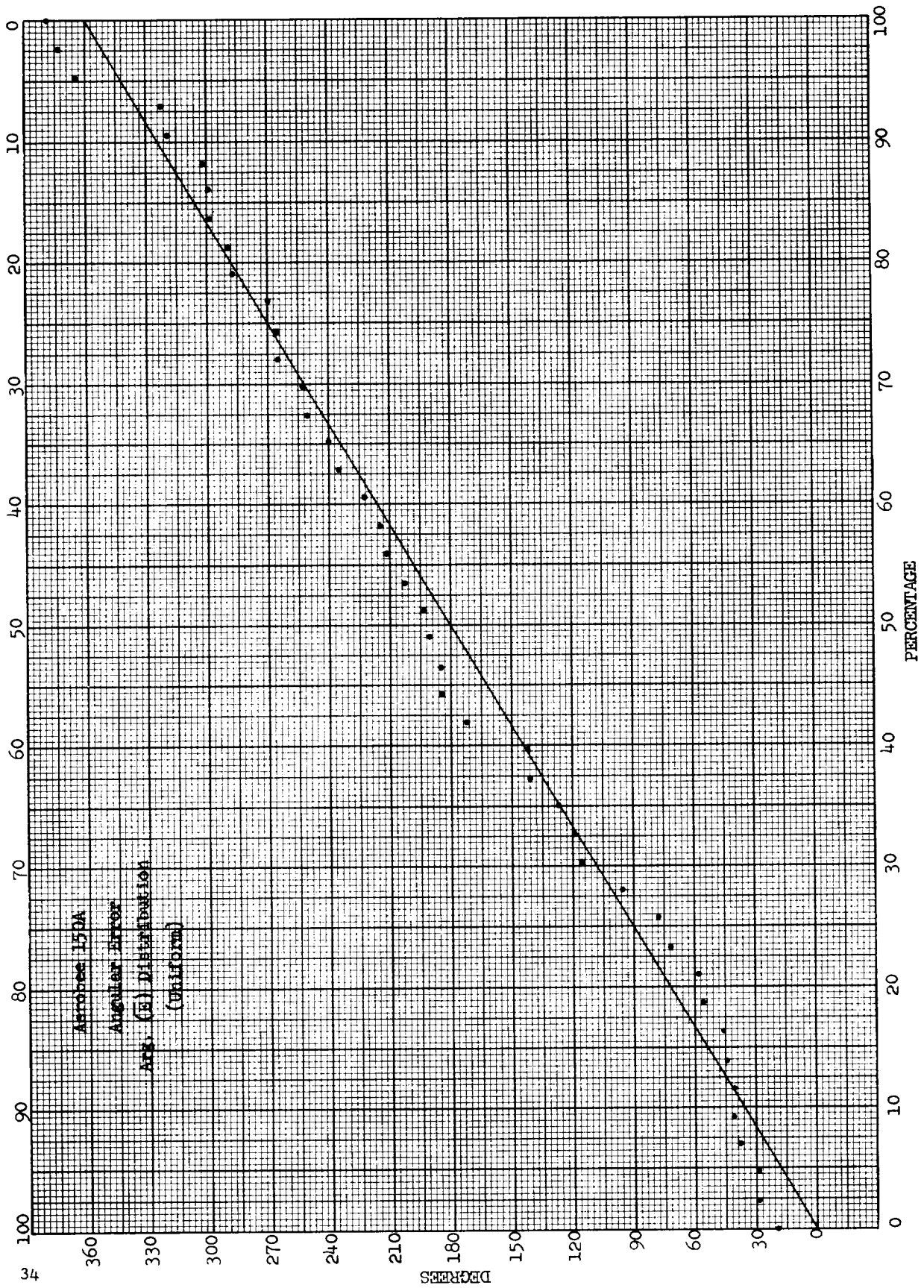
Graph 10



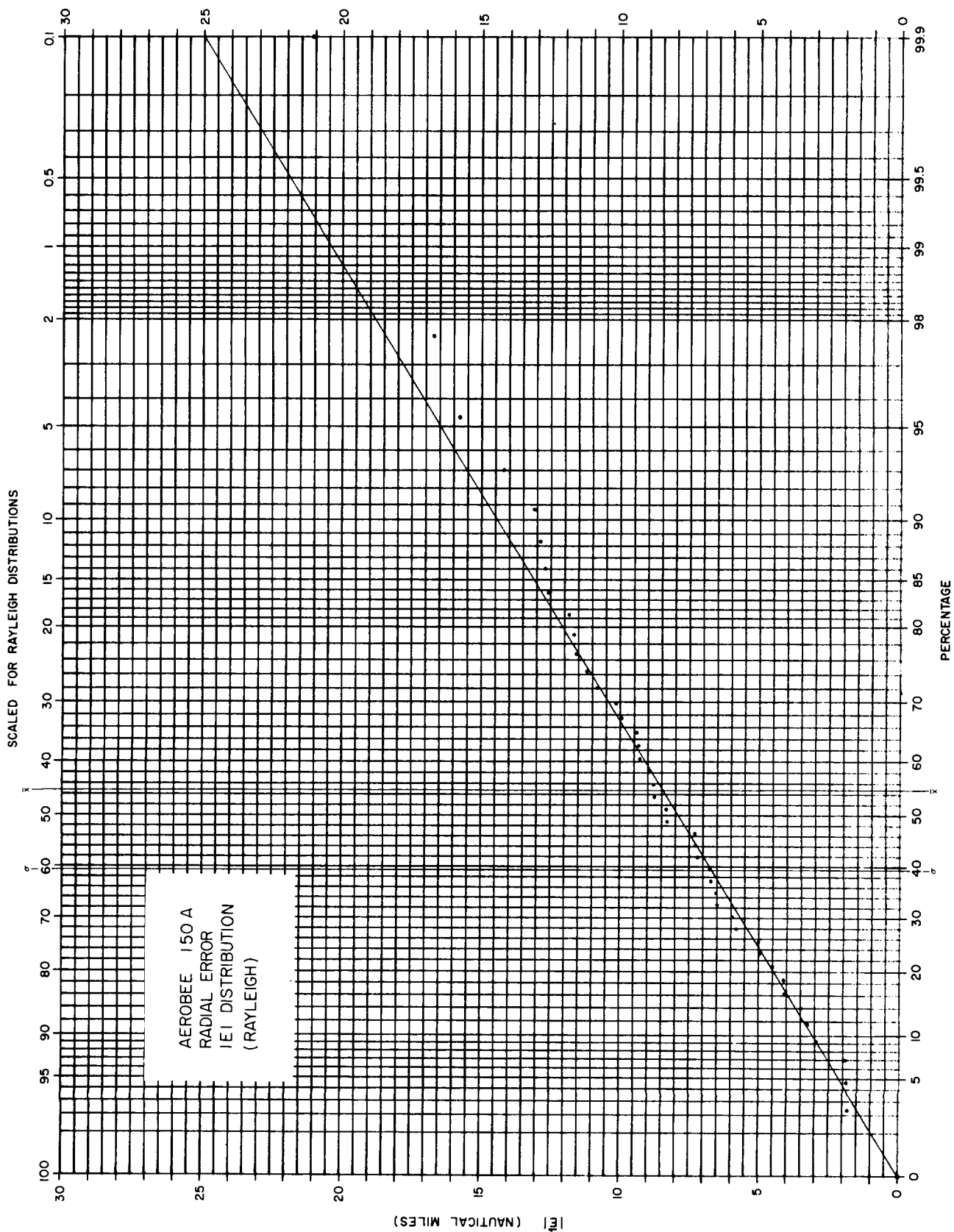
Graph 11



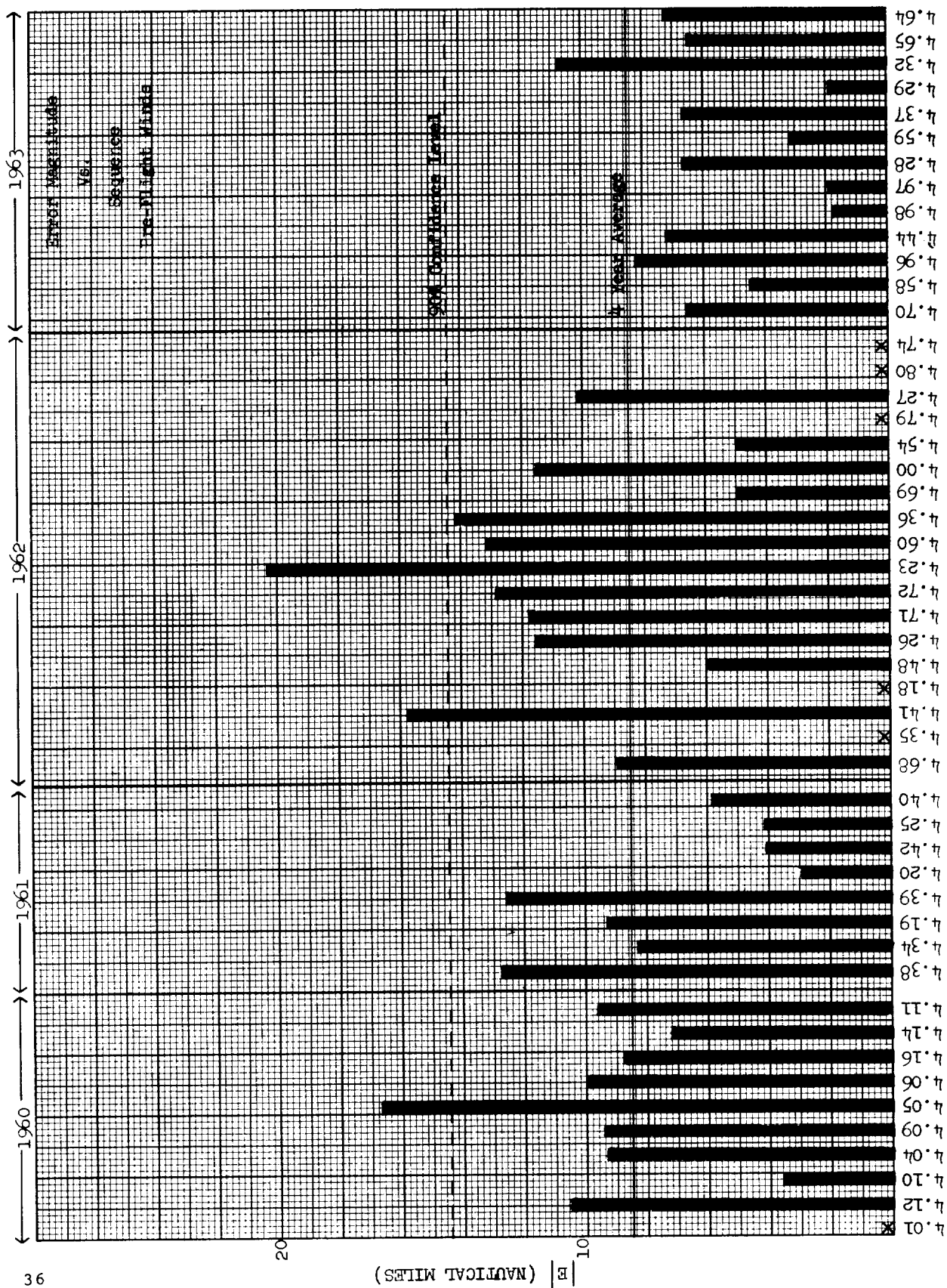
Graph 12



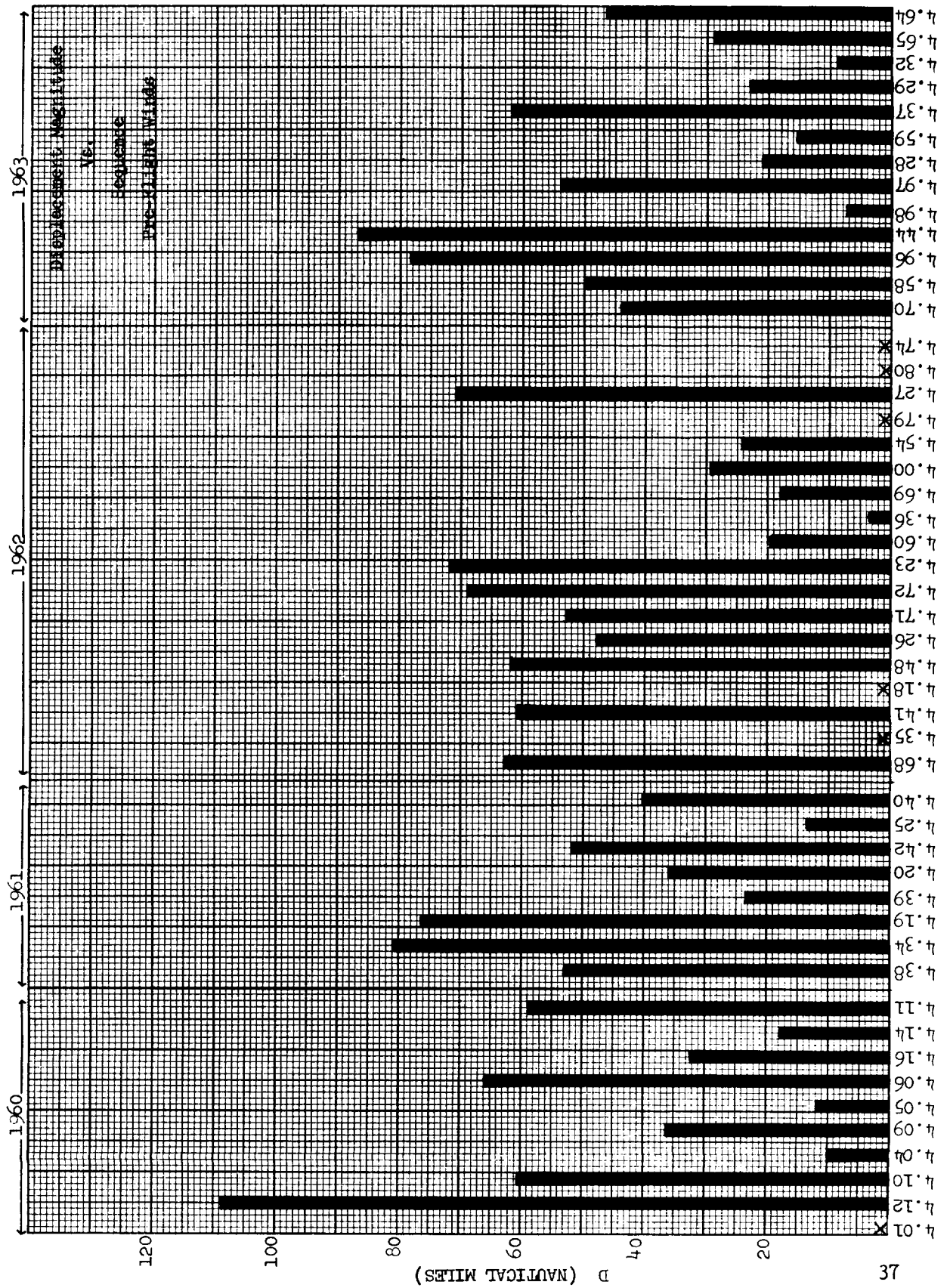
GRAPH 13



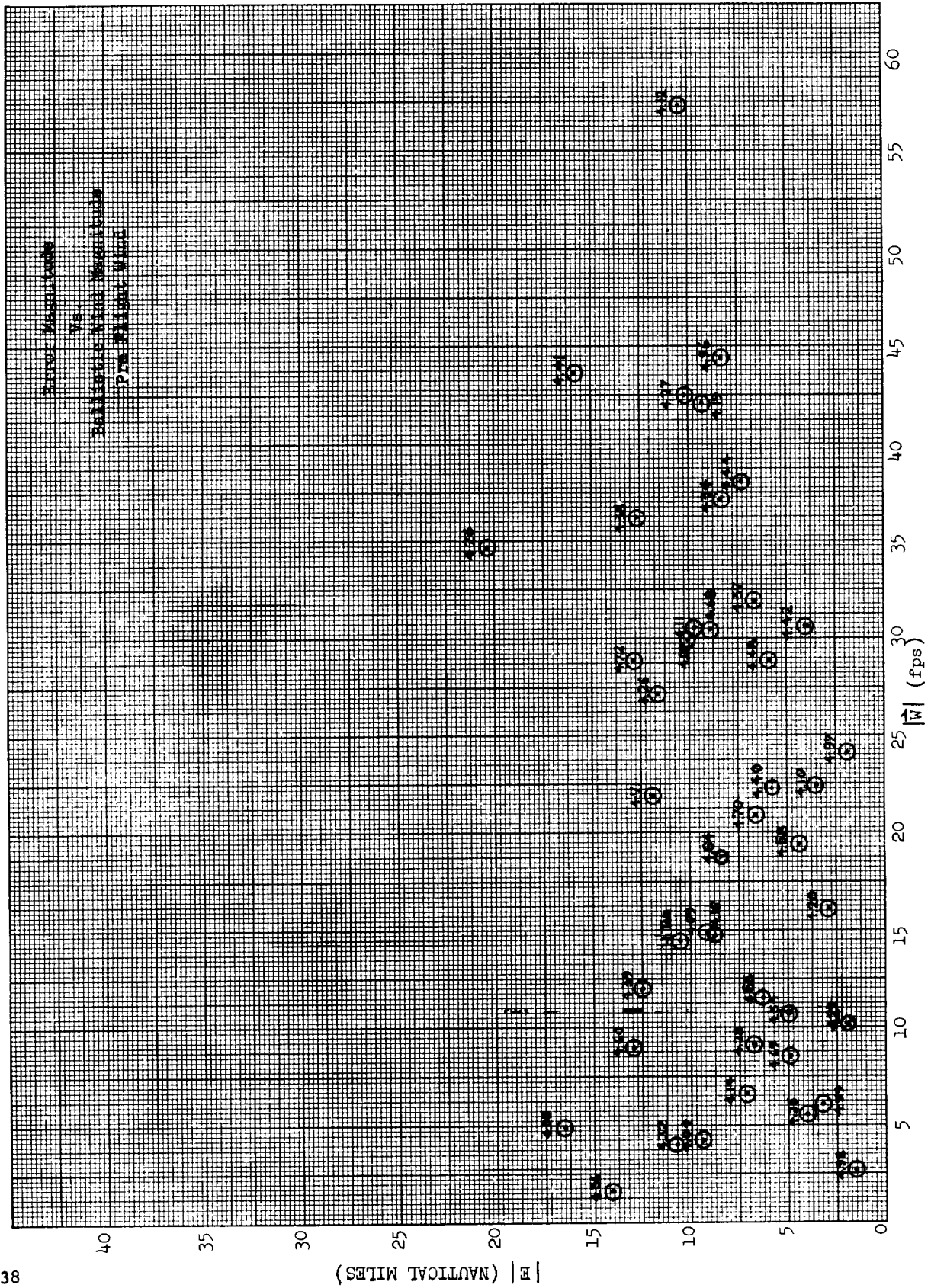
Graph 14

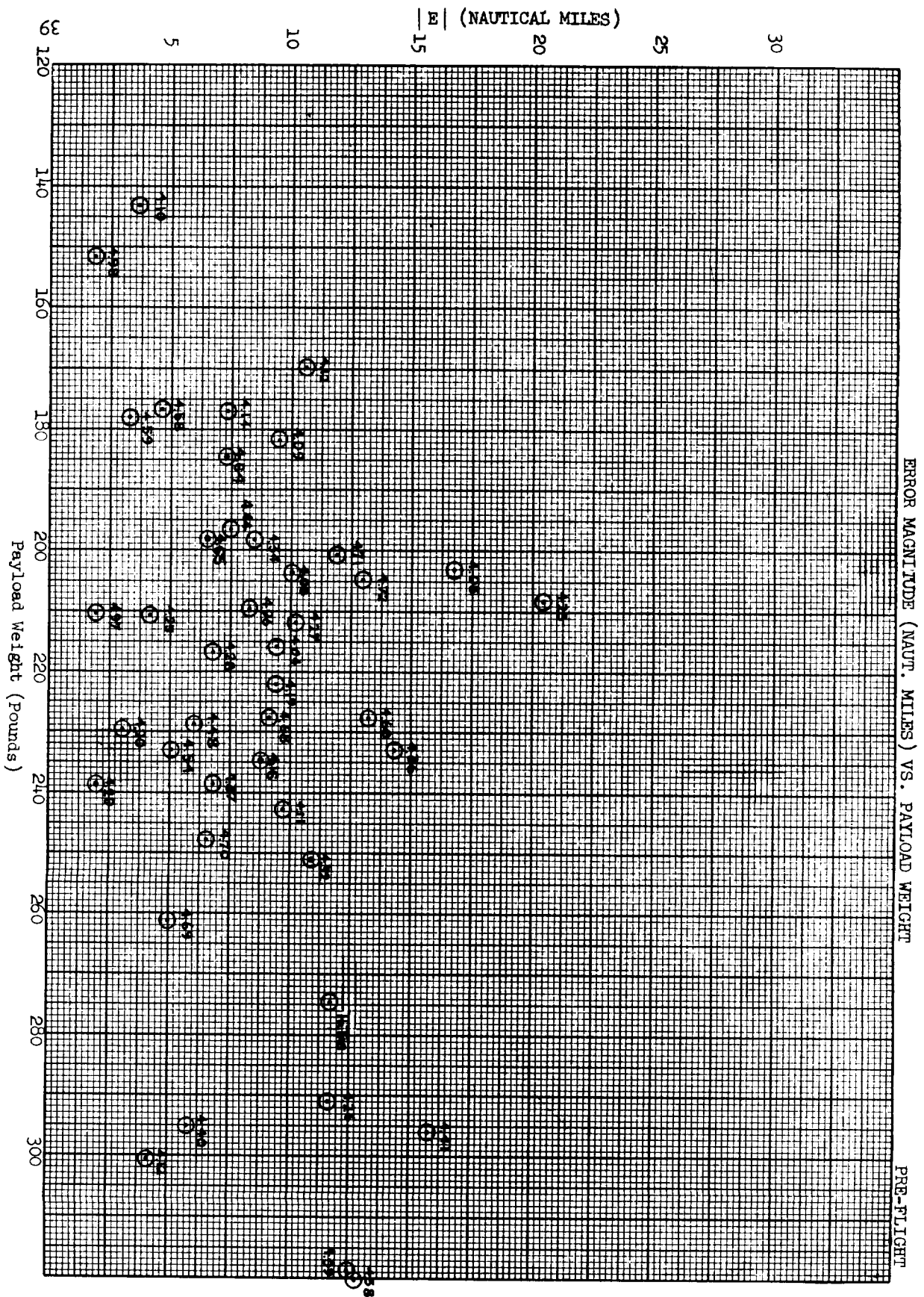


Graph 15



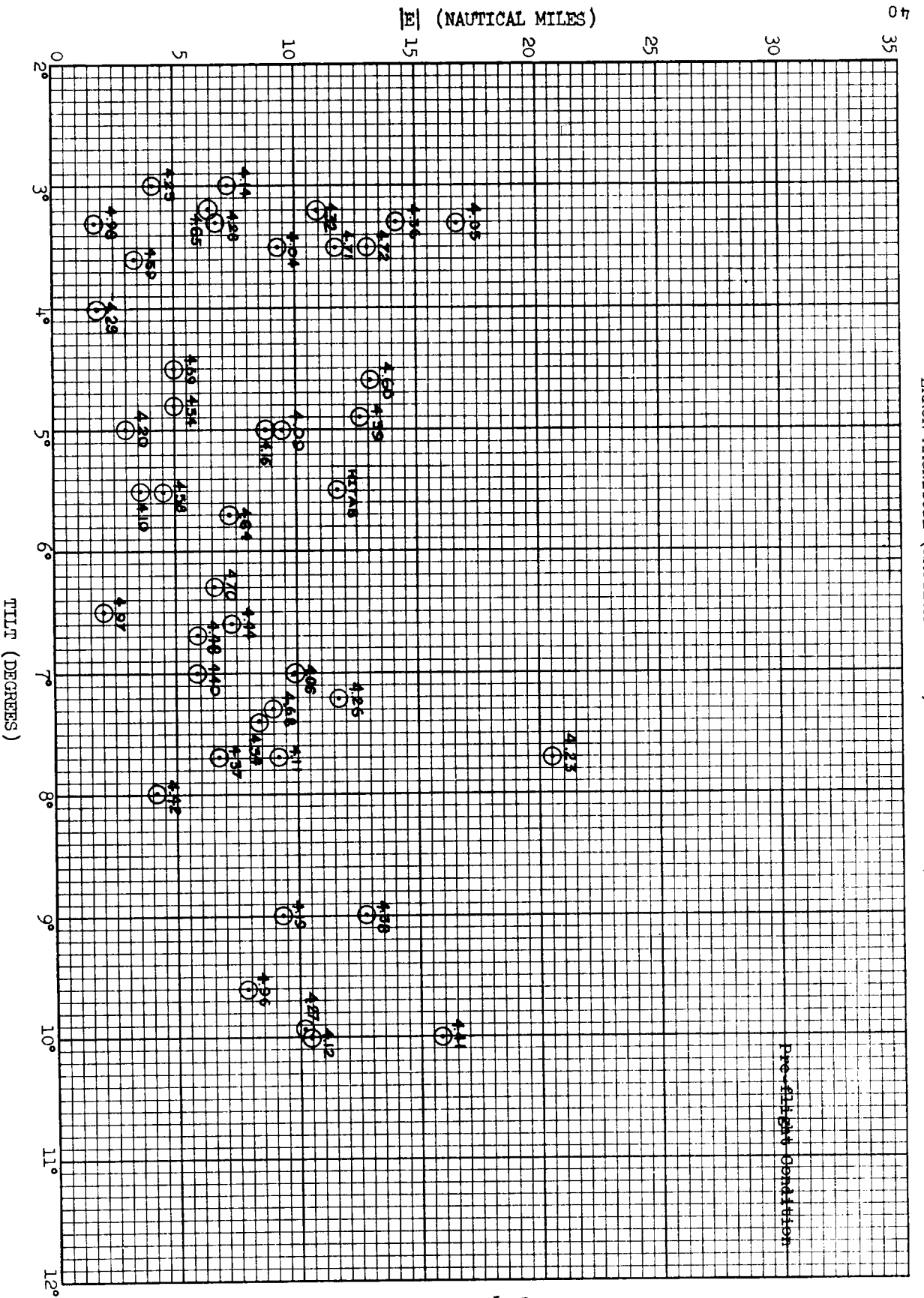
Graph 16



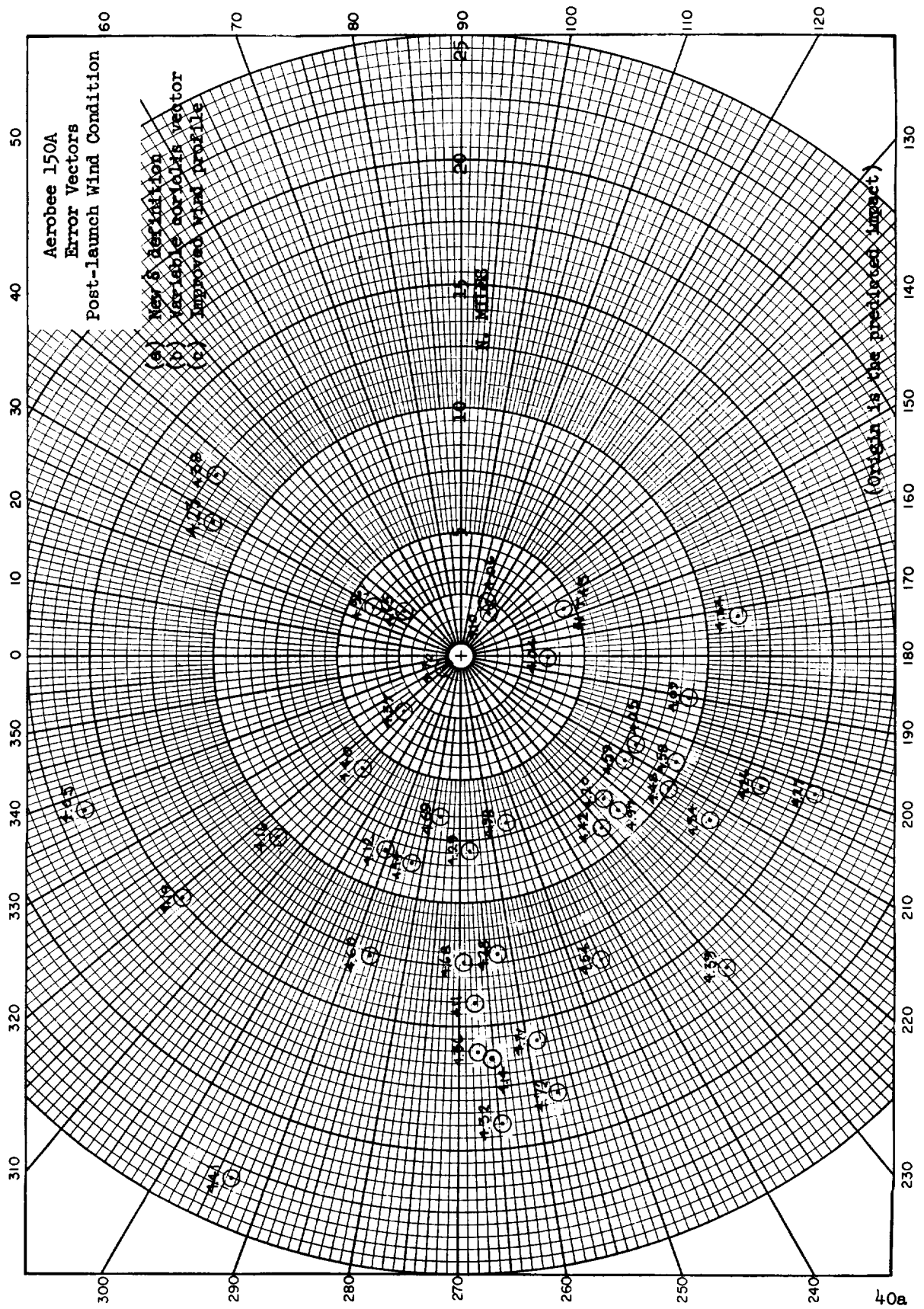


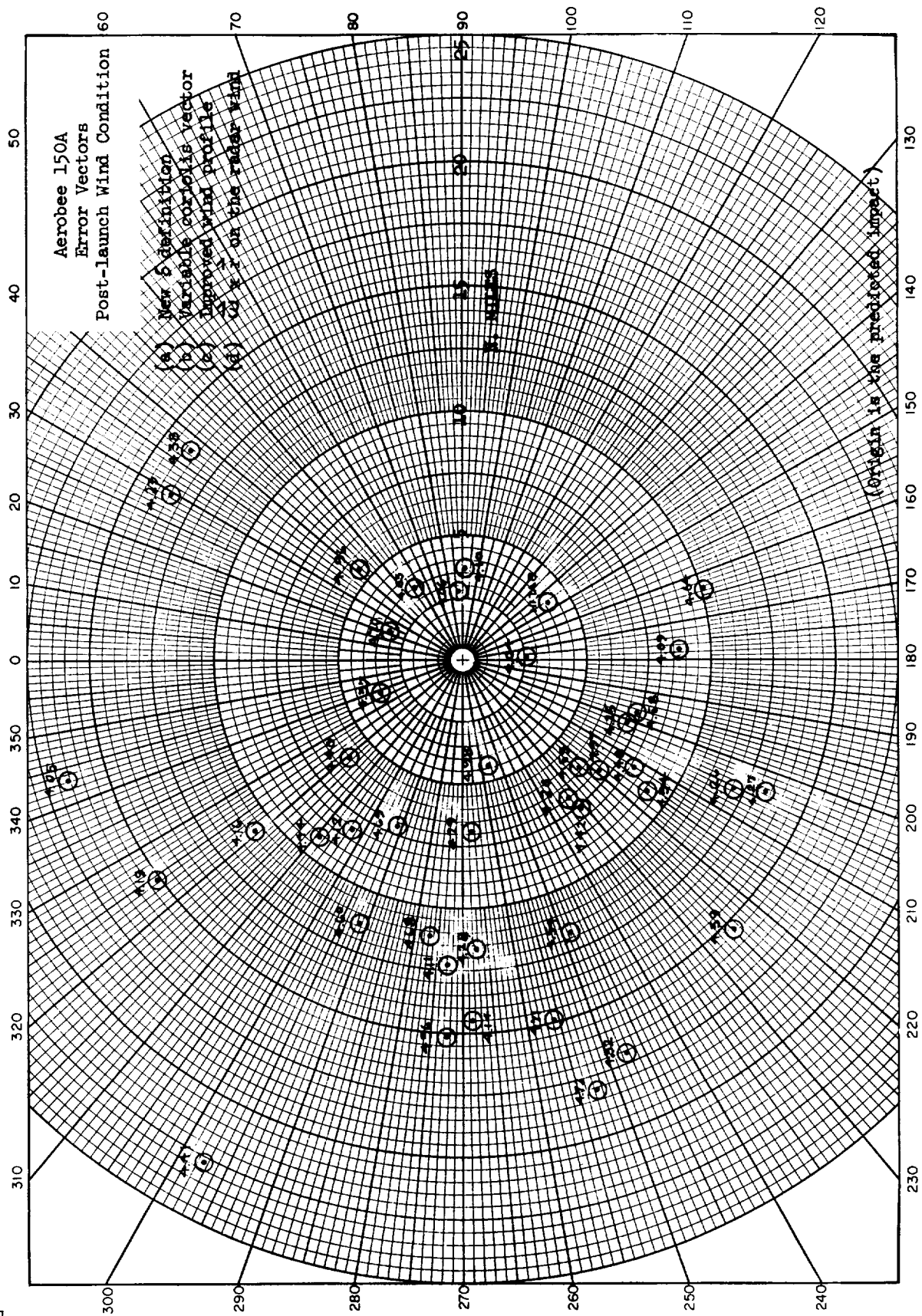
Graph 17

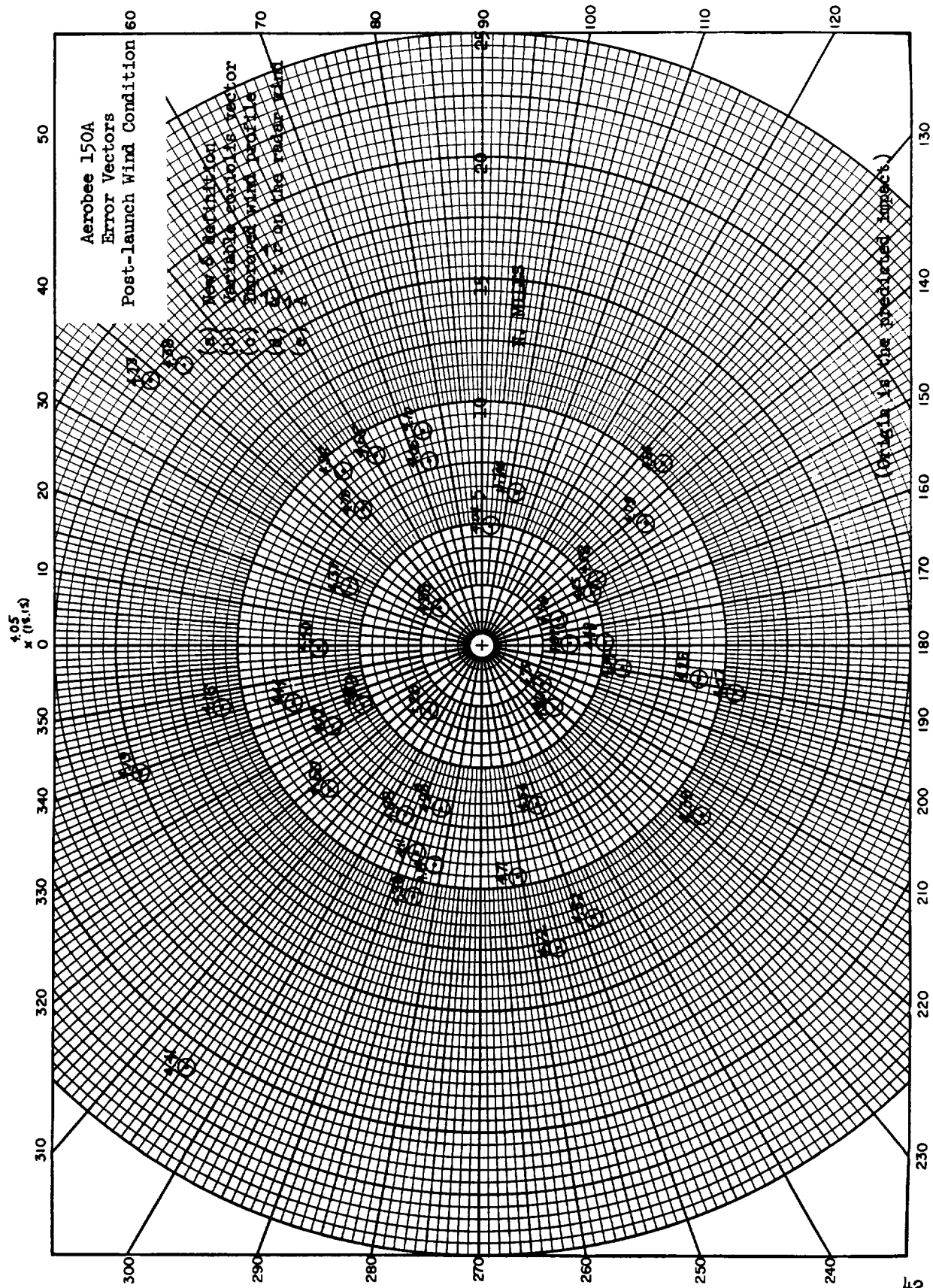
ERROR MAGNITUDE (NAUTICAL MILES) VS. TOWER TILT (DEGREES)

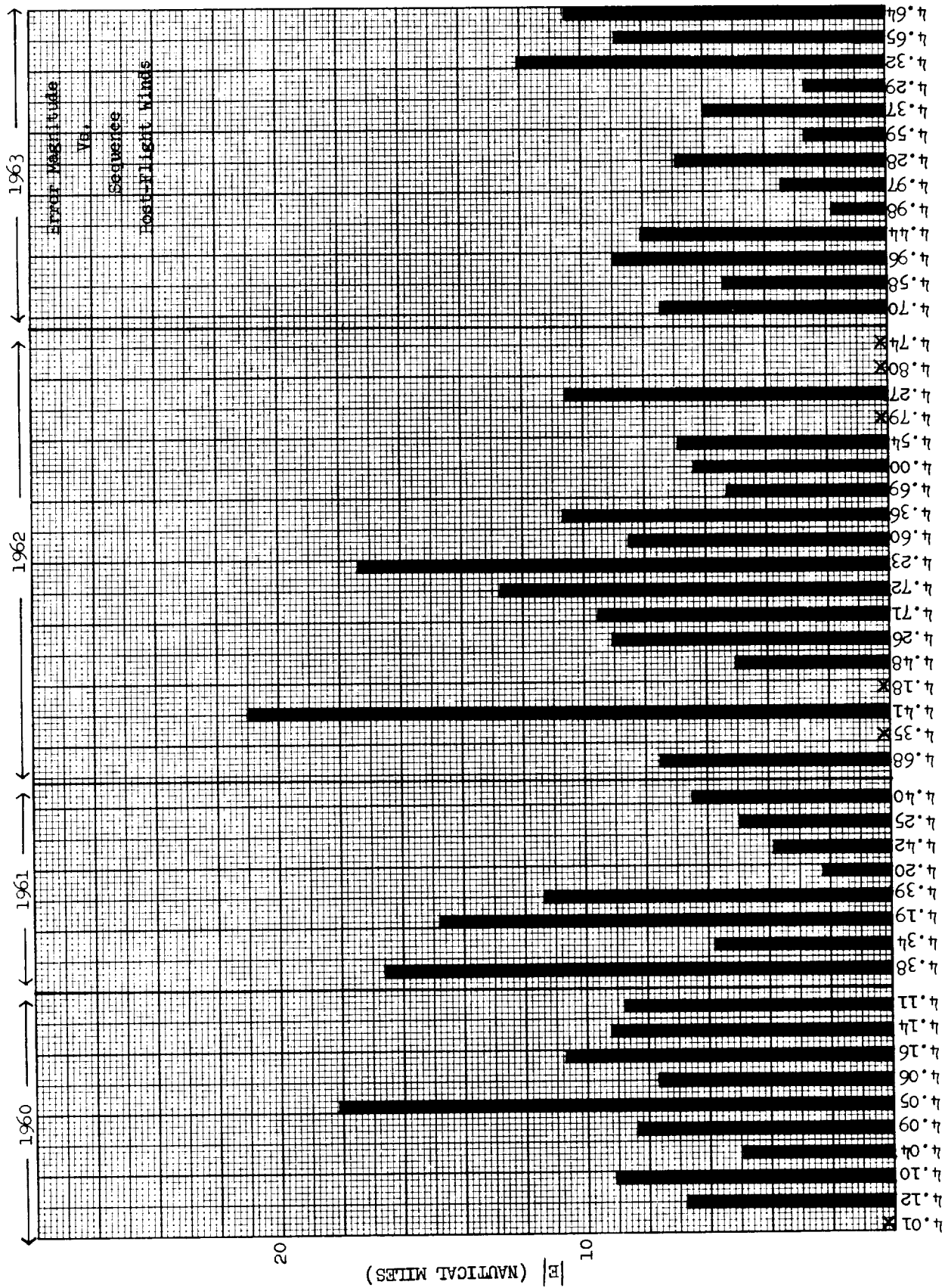


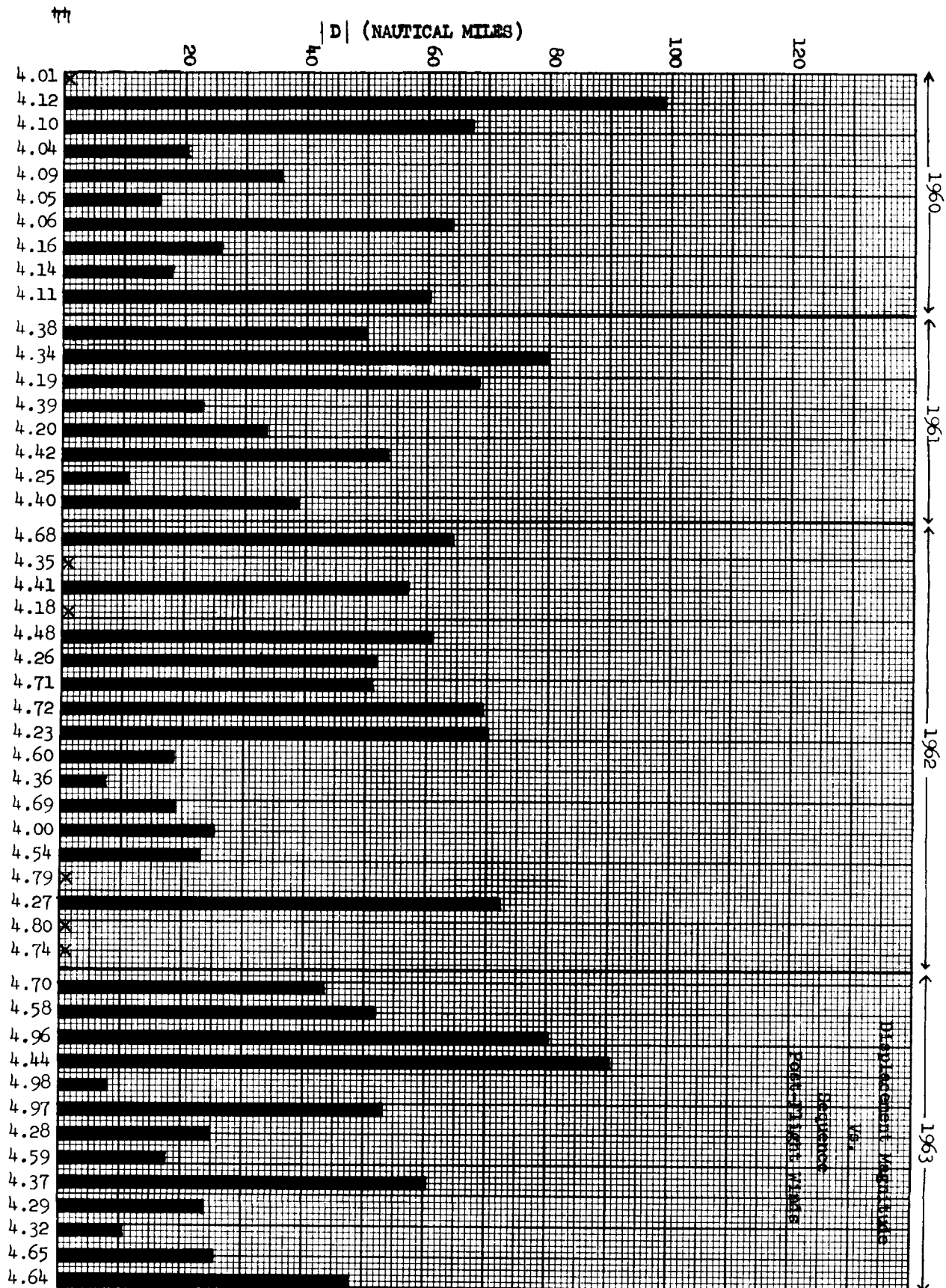
Graph 18

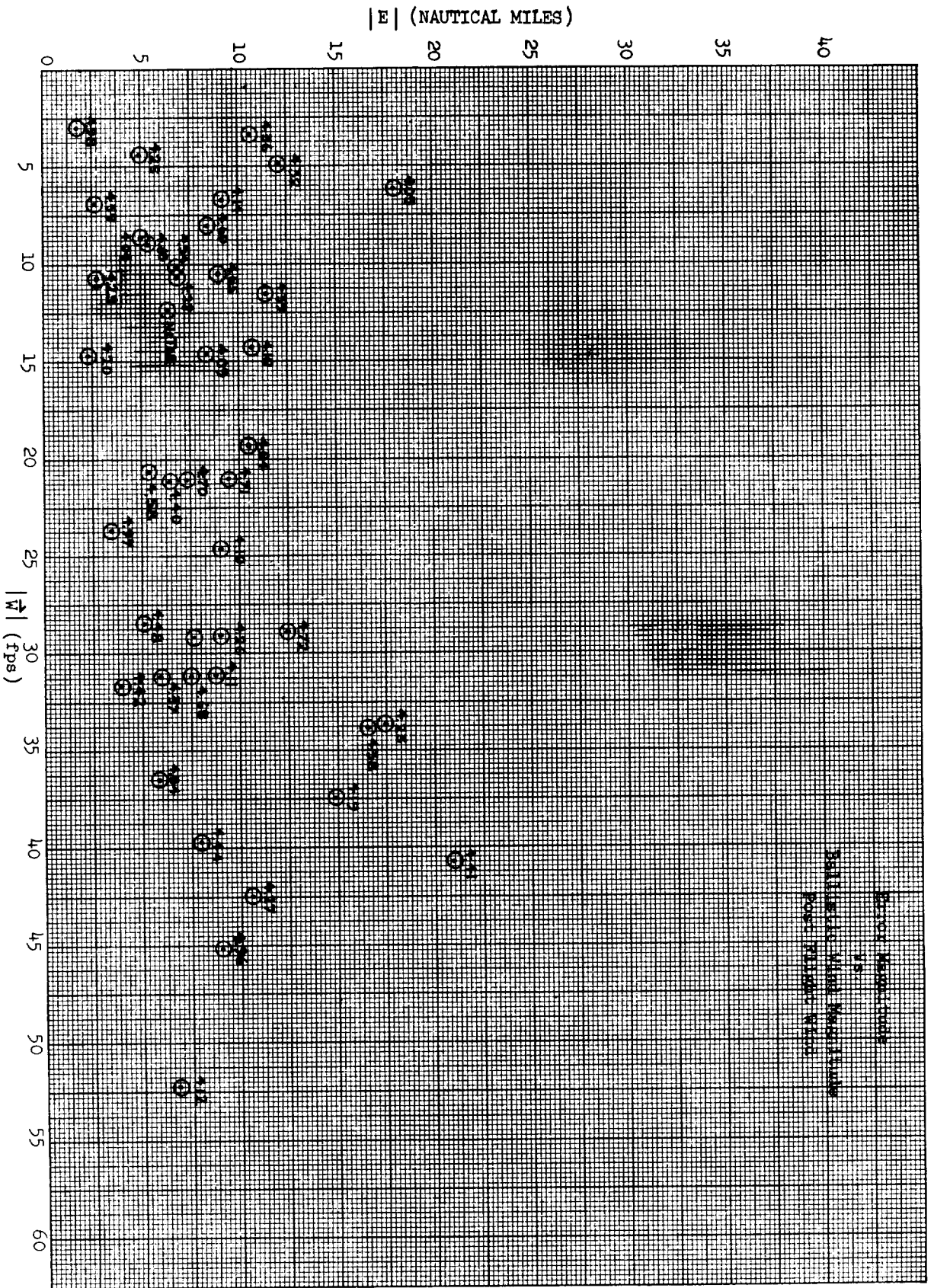






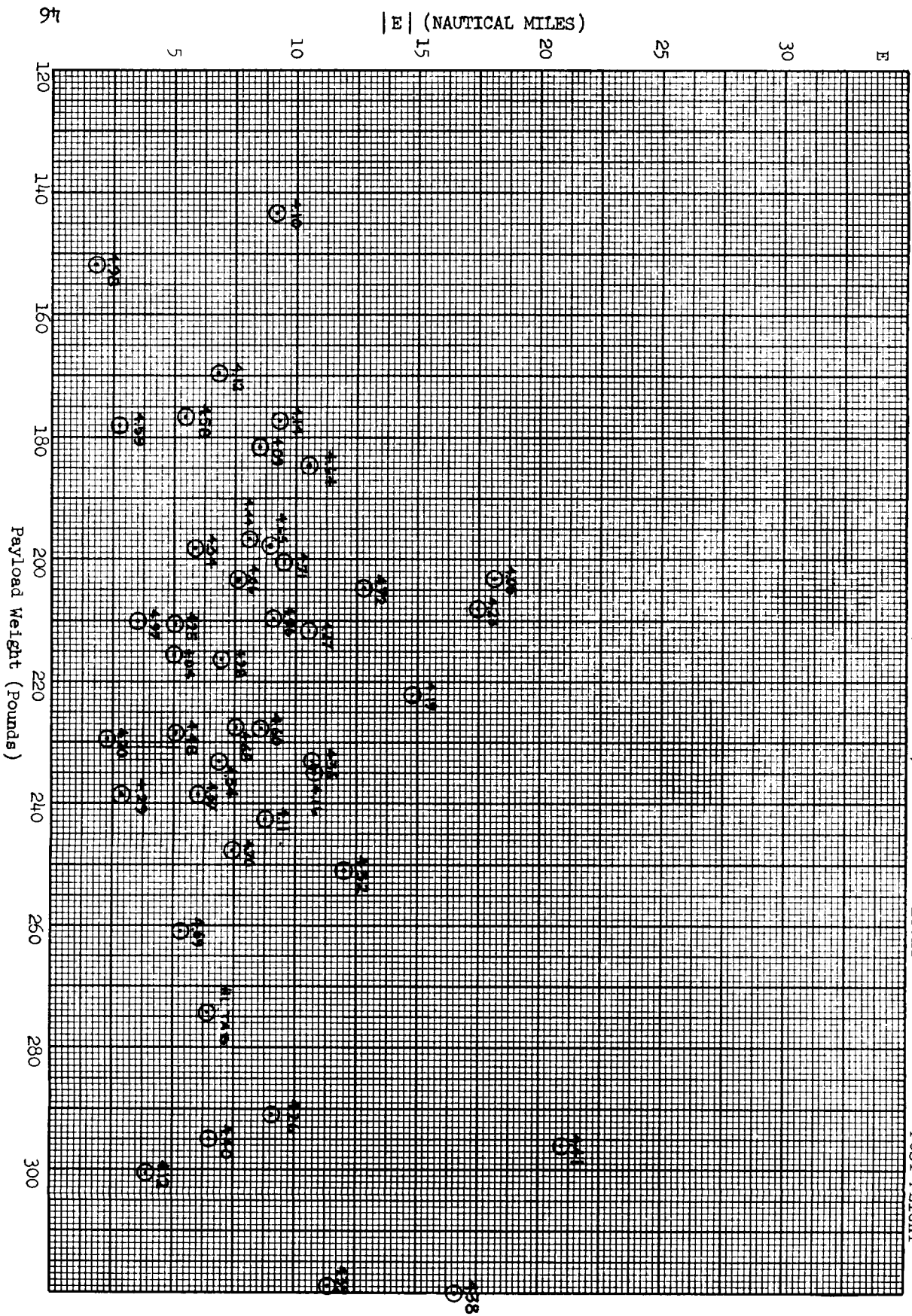




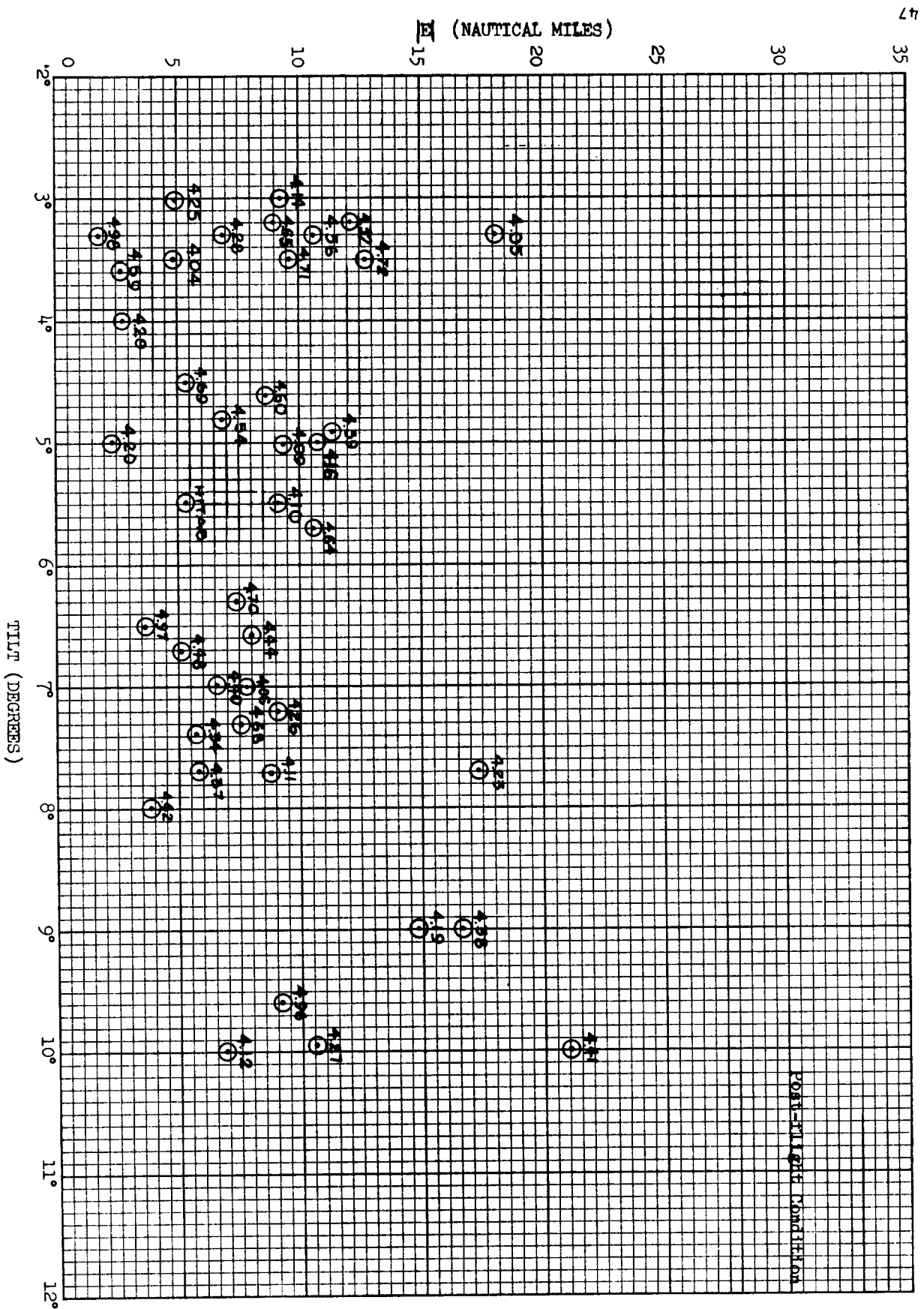


ERROR MAGNITUDE (NAUT. MILES) VS. PAYLOAD WEIGHT

POST-FLIGHT



ERROR MAGNITUDE (NAUTICAL MILES) VS. TOWER TILT (DEGREES)



REFERENCES

1. "Field Wind Weighting and Impact Prediction Procedure for Unguided Rockets." Keith Hennigh, 1 March 1962, Physical Science Laboratory New Mexico State University, University Park, New Mexico.
2. "Vector and Tensor Analysis," Lass, McGraw Hill Book Company, Inc., 1950.

